THE JOURNAL OF PHYSICAL CHEMISTRY A

Article

pubs.acs.org/JPCA

Small Molecules—Big Data

Attila G. Császár,*[,†,‡] Tibor Furtenbacher,[‡] and Péter Árendás[‡,§]

[†]Laboratory of Molecular Structure and Dynamics, Institute of Chemistry, Eötvös Loránd University, P.O. Box 32, H-1518 Budapest 112, Hungary

[‡]MTA-ELTE Complex Chemical Systems Research Group, Pázmány Péter sétány 1/A, H-1117 Budapest, Hungary

[§]Department of Algebra and Number Theory, Institute of Mathematics, Eötvös Loránd University, P.O. Box 120, H-1518 Budapest 112, Hungary

ABSTRACT: Quantum mechanics builds large-scale graphs (networks): the vertices are the discrete energy levels the quantum system possesses, and the edges are the (quantum-mechanically allowed) transitions. Parts of the complete quantum mechanical networks can be probed experimentally via high-resolution, energy-resolved spectroscopic techniques. The complete rovibronic line list information for a given molecule can only be obtained through sophisticated quantum-chemical computations. Experiments as well as computations yield what we call spectroscopic networks (SN). First-principles SNs of even small, three to five atomic molecules can be huge, qualifying for the big data description. Besides helping to interpret high-resolution spectra, the network-theoretical view offers several ideas for improving the accuracy and robustness of the increasingly important information systems containing line-by-line spectroscopic data. For example, the smallest number of measurements necessary to perform to obtain the complete list of energy levels is given by the minimum-weight spanning tree of the SN and network clustering studies may call attention to "weakest links" of a spectroscopic database. A present-day application of spectroscopic networks is within the MARVEL (Measured Active Rotational−Vibrational Energy Levels) approach, whereby the transitions information on a measured SN is turned into experimental energy levels via a weighted linear least-squares refinement. MARVEL has been used successfully for 15 molecules and allowed to validate most of the transitions measured and come up with energy levels with well-defined and realistic uncertainties. Accurate knowledge of the energy levels with computed transition intensities allows the realistic prediction of spectra under many different circumstances, *e.g.*, for widely different temperatures. Detailed knowledge of the energy level structure of a molecule coming from a MARVEL analysis is important for a considerable number of modeling efforts in chemistry, physics, and engineering.

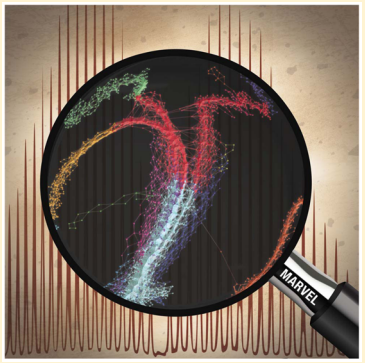

1. INTRODUCTION

Both graph theory, whose more or less definitive start date is 1735, when Euler found an ingenious solution to the Königsberg bridges' problem,[1] and (high-resolution) molecular spectroscopy, whose less well-defined origin can be found in works of Fraunhofer, Kirchhoff (incidentally, a native of Königsberg), Brewster, and Bunsen in the first half of the 1800s,[2] have a rather long history.[3] Around the year 2000 both fields witnessed major shifts in their subjects. Graph theory was extended from the study of small to that of truly large-scale, complex systems.[4−6] These complex networks contain millions and easily billions of nodes and links,[7−13] their analysis often requires algorithms developed for big data. At about the same time, high-resolution molecular spectroscopy witnessed the emergence of more and more complete line lists of molecules,[14−32] containing not thousands but millions and eventually billions of entries, preferably including various spectral line parameters. Atomic spectroscopic databases[33] are just as important for certain modeling studies and they can be quite large, as well.

Complex networks appear ubiquitously in nature, society, communication, and elsewhere.[7] Traditionally, small(er) networks have been examined and interpreted via random graph theory, a mainstay of discrete mathematics developed and popularized by Erdős and Rényi around 1960.[34−36] Distribution of the number of edges, emanating from a vertex, of the Erdős−Rényi random graphs have a well-defined, characteristic mean value, often referred to as a scale. However, about two decades later it became widely recognized that most networks of practical interest do not follow the laws characterizing the Erdős−Rényi random graphs.[7,34,37,38] The first-neighbor degree distributions of most complex natural networks appear to be free of a scale, as emphasized for physicists by Barabási and Albert.[4] Since that pioneering study, a plethora of papers appeared developing the "mathematics" and "physics" of complex networks, both natural and model ones, and finding new occurrences of networks following a degree distribution which can be characterized as scale free.[5] Following studies by Barabási and co-workers,[4,5,8−11,13] it became clear that for a faithful representation of complex systems the random network theory of Erdős and Rényi[34] has to be superseded by that of scaling, including scale-free (SF), random networks.[7]

Received: March 3, 2016
Revised: September 16, 2016
Published: September 27, 2016

DOI: 10.1021/acs.jpca.6b02293
J. Phys. Chem. A 2016, 120, 8949−8969

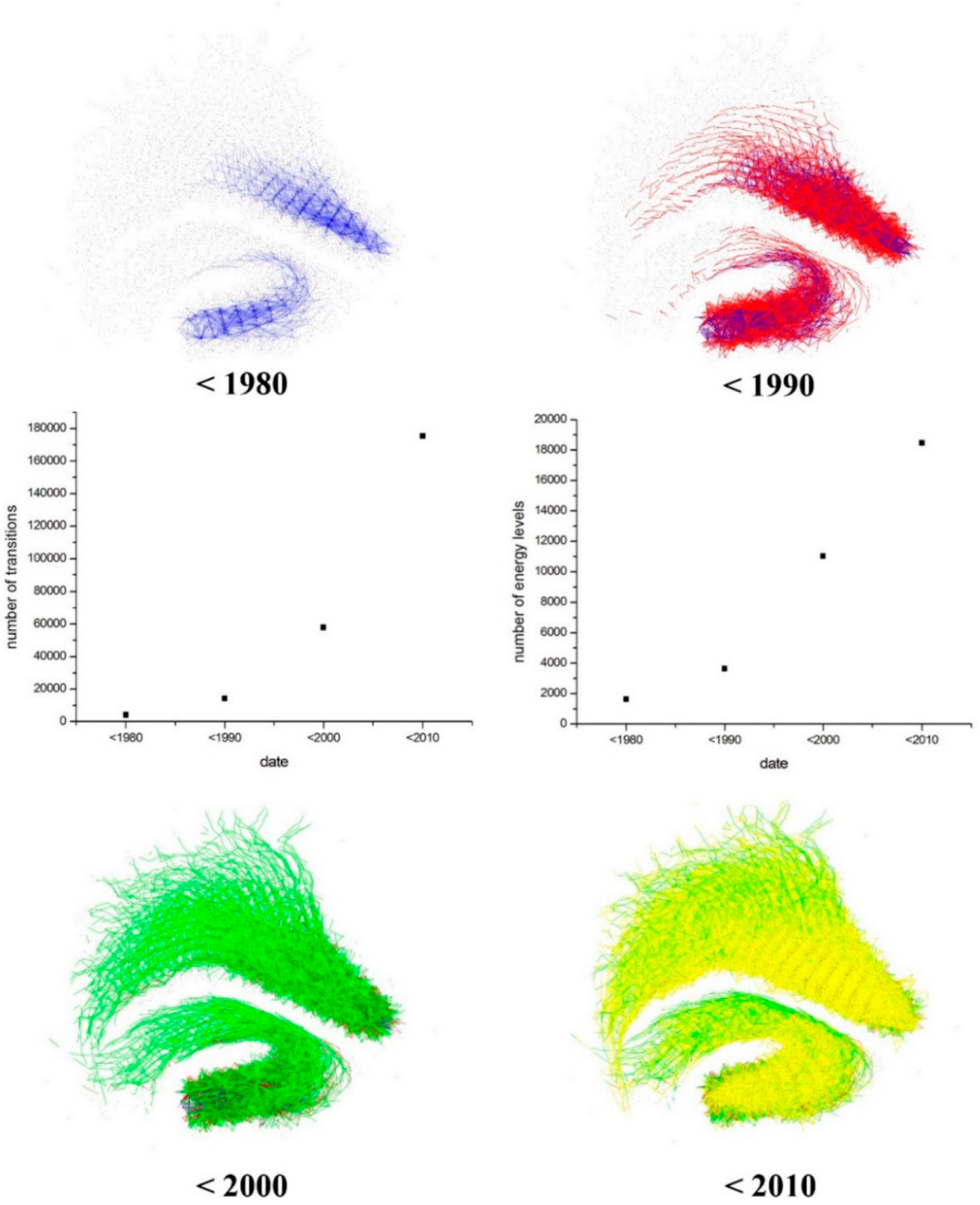

Figure 1. Decade-by-decade temporal development of the experimental spectroscopic network (SN) of $H_2{}^{16}O$. The shape of SNs can be drawn arbitrarily; the representation selected here emphasizes the most important characteristics of the experimental SN of $H_2{}^{16}O$. The visual information is augmented in the middle of the figure with the decade-by-decade expansion of the number of measured transitions and energy levels. The transitions measured in the different time intervals are indicated in the panels with different colors, the later measurements are drawn on top of the earlier ones. The separate *ortho*- and *para*-$H_2{}^{16}O$ components, *ortho* being the larger one due to the effect of nuclear spin statistics on the measured intensities, are clearly visible. Note, in particular, the more-or-less quadratic increase in the number of measured and assigned transitions accompanied by only a more-or-less linear increase in the number of experimentally known energy levels.

Complete characterization of high-resolution rotation−vibration−electronic (rovibronic) spectra of a considerable number of molecules, the only quantum systems considered here, starting from the microwave and extending to the ultraviolet, is a prerequisite for modeling and understanding of many processes and phenomena relevant in physics, chemistry, and engineering. Modellers of the atmospheres of planets and cool stars as well as those investigating combustion in rocket exhausts and turbine engines need detailed and accurate temperature-dependent line-by-line information, which not

DOI: 10.1021/acs.jpca.6b02293
J. Phys. Chem. A 2016, 120, 8949−8969

even the most elaborate spectroscopic measurements can provide (for example, at elevated temperatures). In statistical theories of chemical reaction rates, a central role is assumed by the density of (ro)vibrational states.[39] The experimental determination of the density of states and its integral, the total number of accessible states, is a formidable challenge at high(er) energies for all but the smallest molecules. Recent advances in high-resolution molecular spectroscopy led to a considerable increase in the extent of related experimental spectroscopic information. Some of the data have been deposited, sometimes in a critically evaluated and annotated form, in databases.[17−32,40−43]

As an example, Figure 1 shows the temporal development of our experimental understanding of the rovibrational energy level (and transition) structure of the lowest electronic state of the $H_2{}^{16}O$ molecule, based on data collected in ref 42. As usual for graphs, the positioning of the vertices and edges of Figure 1 is completely arbitrary. The overlap of the color-coded rovibrational transitions of Figure 1 show how the number of experimental transitions that have been measured and analyzed grew decade by decade until it reached our present understanding, with about 20000 experimental energy levels deduced from about 200000 experimental transitions.[42] Treatment of the rapidly increasing information and the desire to turn information into knowledge requires sophisticated procedures in the generation, accumulation, validation, handling, visualization, and distribution of spectroscopic data.

The result of a spectroscopic measurement is almost always a set of experimental transition wavenumbers and transition intensities for a given wavenumber range, covering selected parts of the energy eigenstates. It is feasible to publish such an experimental list and compare the results with those of previous reports through effective spectroscopic constants describing these transitions with experimental accuracy. The assignment procedure is sped up, and the results are more clearly embedded in the set of existing data if one can access a database with the complete set of existing transition wavenumbers and energy levels and use the combination differences procedure. However, this has rarely been done in the past. This is a significant problem in high-resolution spectroscopy as there is an unusually large number of inherent interdependencies among the energy levels and the transitions, most of which are ignored in the traditional approach. There are several further notable disadvantages related to the traditional way spectroscopists have been assigning their measured high-resolution spectra. These disadvantages often transform into significant problems when the data are deposited in spectroscopic databases. It is worth reviewing here some of these hindrances of the traditional approach.

There are only a few good quantum numbers[44] characterizing the energy levels involved in the measured transitions. Most of the quantum numbers used to describe the states are approximate[44] ones. Creation of a database where the energy levels are labeled with approximate quantum numbers, independently of how meaningful the quantum numbers are, assures that a unique and complete set of experimental energy levels can be built.[45−47] Nevertheless, the approximate nature of the quantum numbers may become a significant problem when a large number of scientists contribute to the understanding of the experimental rovibronic states of a molecule, this being the usual case, as they tend to use different, often conflicting approximate quantum numbers (*e.g.*, local vs normal mode labels for the vibrations and the different labeling possibilities for symmetric and spherical tops, especially when contortional motions[44] are allowed). The problem is exacerbated at higher excitations when it usually becomes completely unfeasible to provide physically meaningful labels.

If there are only a few rovibrational transitions measured for a given vibrational parent, construction of a reliable effective Hamiltonian is significantly hindered. This may be the case, for example, when the measurement is based on the use of a single narrow laser source. There may certainly be a difference between the accuracy and the precision of the energies when only a small portion of a spectrum is analyzed. Determining the accuracy of measurements processed via the traditional approach may be misleading. Lacking the details provided by a global analysis of all measurements may allow the declaration of much too small uncertainties, the incompatibility of the uncertainties attached to the transitions and the underlying energy levels may become unrealistic.

Finally, in an ideal world with zero uncertainties in the measurement results, knowledge of N connected nonzero rovibronic energy levels would require N measurements (it is natural to take the lowest energy level as zero). However, as the entries of Table 1 exemplify, the usual spectroscopic practice is very far away from this situation: it happens that 10 times as many transitions are measured than energy levels determined. Thus, how to best utilize all the measurement results and how to minimize unnecessary and costly experimental efforts seems to be an overly important task in high-resolution spectroscopy.

Table 1. Selected Data, Including the Number of Experimentally Identified and Subsequently Validated Transitions and the Resulting MARVEL Energy Levels, about Experimental Spectroscopic Networks of Small Molecules

		measured transitions			
species	ref	identified	validated	energy levels	no. of sources
$^{12}C_2$	59	23343	22949	5699	39
H_3^+	56	1610	1410	652	26
H_2D^+	57	195	185	109	13
D_2H^+	57	154	136	104	9
$H_2{}^{16}O$	42	184667	182156	18486	93
$H_2{}^{18}O$	40	32325	31705	5131	48
$H_2{}^{17}O$	40	9169	9028	2723	33
$HD^{16}O$	41	54740	53291	8818	74
$HD^{18}O$	41	8729	8634	1864	18
$HD^{17}O$	41	485	478	162	3
$D_2{}^{16}O$	43	63050	62372	12301	74
$D_2{}^{18}O$	43	12163	12018	3351	18
$D_2{}^{17}O$	43	600	583	338	3
$^{14}NH_3$	58	29450	28530	4961	56
$H_2{}^{12}C{}^{12}C{}^{16}O$	55	3982	3194	1722	12

These problems are realized immediately when spectroscopic databases are upgraded with the latest information, which happens on a regular basis with, for example, the canonical HITRAN database.[24] Each time a large set of corrections is introduced, they improve the overall quality of the database but it often remains unclear to the user which data are responsible for the previous problems and the corrections. The rapid growth of measured transitions and the much less rapid evolution of our knowledge about the energy level set can also be traced back to shortcomings of the traditional, serial approach to high-resolution spectra and spectroscopy.

DOI: 10.1021/acs.jpca.6b02293
J. Phys. Chem. A 2016, 120, 8949−8969

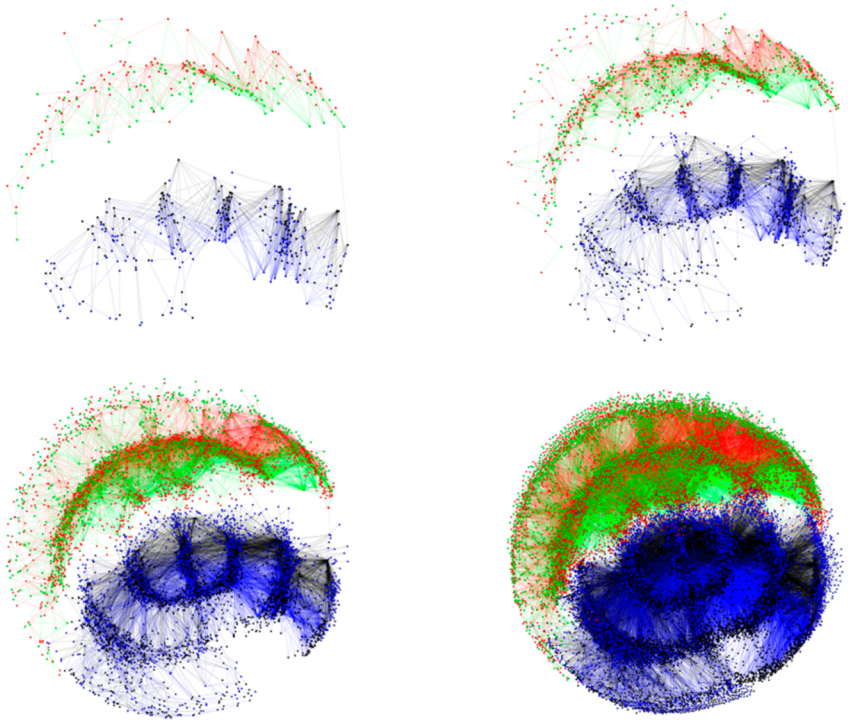

Figure 2. Visual representation of first-principles one-photon absorption spectroscopic networks of $H_2{}^{16}O$ obtained with transition intensity cutoffs, from left to right, of 10^{-20}, 10^{-22}, 10^{-24}, and 10^{-26} cm molecule^{-1}. The two principal components and the bipartite character of the network are clearly visible, as well as the development of hubs (energy levels with an unusually large number of transitions) within the network.

Considering all the interdependencies of all the measurements all at the same time seems to be the answer to almost all of the problems mentioned. This provides a way to an improved error and uncertainty analysis, a much improved facility to determine the overall accuracy of the complete set of measurements, a clear recipe to provide accurate uncertainties, covariances, and provenances, while allowing us to utilize all the measurements that have dependable uncertainties independent of whether they are small or large.

It is the belief of the authors that in search of useful novel tools for validating and improving energy levels and transitions within spectroscopic line lists, as well as improving the understanding of the underlying experiments, network theory and its sophisticated polynomial algorithms offer interesting and highly useful possibilities, some of which are described and explored below.

This belief is based on the fact that for individual molecules quantum mechanics (QM) offers a simple, natural, and elegant way to build large-scale networks. The QM networks are made up of energy levels, forming nodes (vertices), while the allowed transitions between the levels form links (edges).[48−54] It is feasible to characterize QM networks experimentally via high-resolution techniques of molecular spectroscopy.[40−43,55−60] Thus, the term *spectroscopic network* (SN) was introduced[48] for practical realizations of QM networks. The robust organizing principle of SNs is provided by QM selection rules; different transitions and transition intensities characterize different spectroscopic techniques. Even for the experimentally most thoroughly studied molecules the observable transitions form just a tiny part of all the allowed transitions.[42,58,60] The complete list of allowed transitions can only be determined via sophisticated fourth-age quantum chemical computations.[61−64] Different intensity cutoffs for the transitions can be used to build first-principles SNs of different size.[52] Figure 2 shows the visual representation of four such first-principles SNs of $H_2{}^{16}O$, corresponding to 298 K one-photon absorption spectra with transition intensity cutoffs of 10^{-20}, 10^{-22}, 10^{-24}, and 10^{-26} cm molecule^{-1}. The data employed to generate Figure 2 are available in ref 42. The components corresponding to *ortho*- and *para*-$H_2{}^{16}O$ are clearly visible in Figure 2, as well as the buildup of vertices with a large number of edges, called hubs (section 2).

Viewing high-resolution molecular spectra as networks (Figure 3, *vide infra*) helps to answer a number of important as well as intriguing questions, some of which address shortcomings of the traditional, serial spectroscopic approach mentioned, including the following:

(1) What would be the most economical way, *i.e.*, the one based on the smallest number of feasible measurements, to determine the complete set of rovibronic states of a molecule?
(2) What is the best way to validate existing spectroscopic measurements and to guide the design of future ones if efficiency is of prime concern?
(3) Could one order the energy levels of a molecule based on their "importance", and could we determine those transitions whose *accurate* knowledge is most important for improving the true accuracy of experimental line lists and related information systems?
(4) How could experimental and theoretical high-resolution spectral data be unified and how could first-principles data be used to simplify the assignment of measured spectra?

The steps leading to answers to these questions require the understanding of the structure of SNs. For example, we need to know how many components would an experimental and a first-principles spectroscopic network possess. Then, we must

DOI: 10.1021/acs.jpca.6b02293
J. Phys. Chem. A 2016, 120, 8949−8969

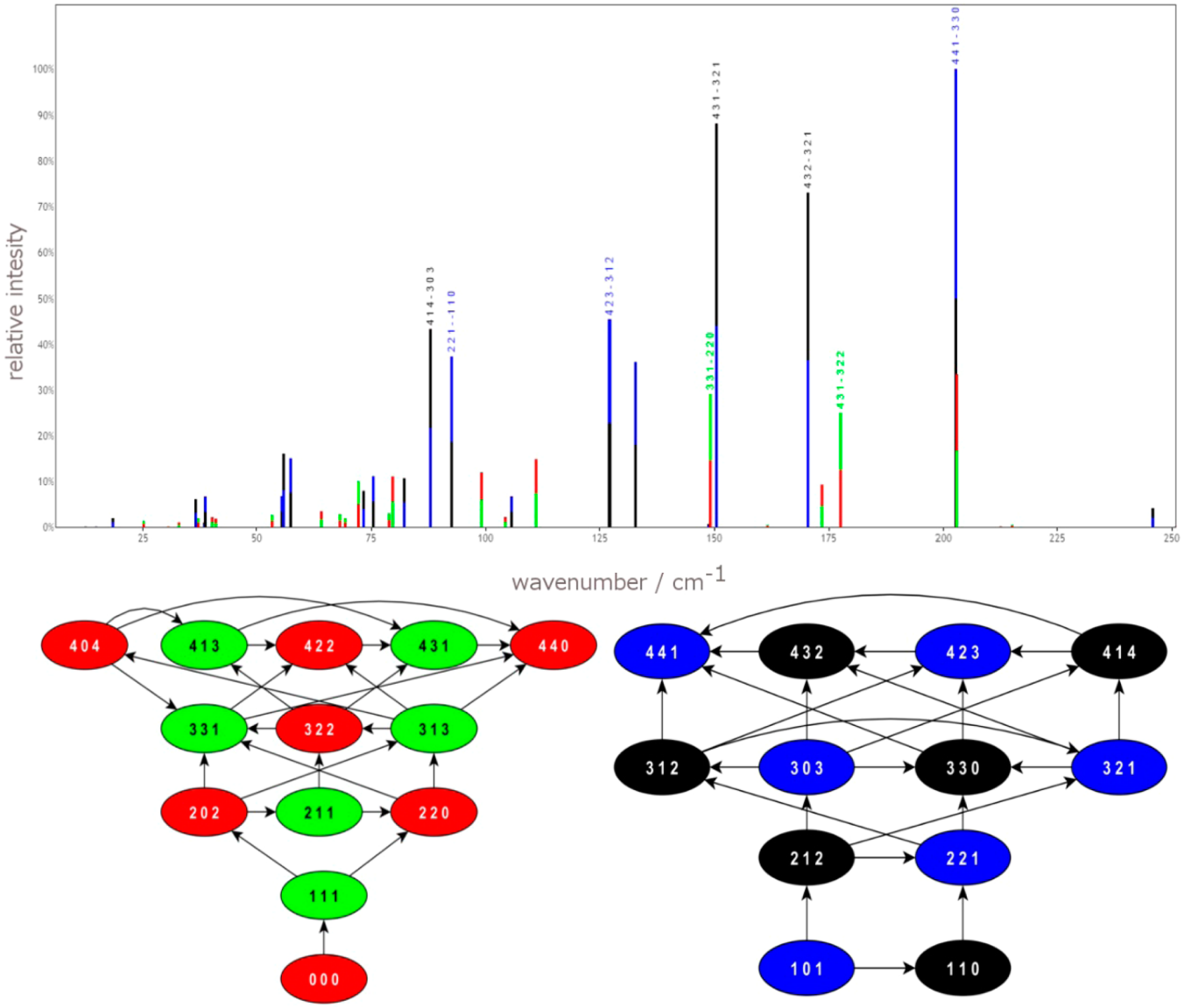

Figure 3. Connection between the pure absorption rotational spectrum of $H_2{}^{16}O$ corresponding to the ground vibrational state (upper panel) and the two components of the spectroscopic network (lower left and right panels, corresponding to *para*- and *ortho*-$H_2{}^{16}O$, respectively) these observable transitions determine. The standard rotational J K_a K_c quantum number assignment is indicated both in the spectrum and in the ovals, representing the energy levels. The two-component bipartite nature of the spectrum is emphasized by the applied coloring (see the text for further details). The arrows point toward the upper state involved in a given transition.

understand whether the structure of an experimental SN is such that it supports only small components or it is characterized by a giant component or perhaps a few of them. We also need to know if any of these components, small or large, have any special structure; in other words, would the various selection rules of molecular spectroscopy dictate any special structure for the experimental and/or first-principles SNs? Furthermore, what kind of degree distribution would the links in the components of an experimental SN follow and would this be different from the distributions observable in the corresponding (truncated) first-principles SNs? How about not only first but also second and higher degree distributions?

It is certainly clear that interpretation and validation of the results of high-resolution spectroscopic experiments via network theory help to improve the accuracy, completeness, and robustness of line lists and guide related experiments. It is noted in this respect that having complete and accurate line lists for molecules of, for example, atmospheric and astrophysical interest at arbitrary temperatures is one of the "holy grails" of modern applied high-resolution spectroscopy. It is also important to emphasize the complementary nature of first-principles and measured line lists: although the relative accuracy of even the best first-principles energy levels is some 10−10000 times worse than that of typical experimental high-resolution transition data, most of the computed transition intensities have accuracies similar to those of experimental data. Thus, for the foreseeable future one needs to consider the combination of experimental and *ab initio* information to satisfy the needs of modellers.

The rest of the paper is organized as follows. Section 2 provides the graph-theoretical foundation necessary for the discussions in the subsequent sections of the article. Section 2 can be skipped by those familiar with at least the elementary ideas of modern network theory. Section 3 provides a detailed

DOI: 10.1021/acs.jpca.6b02293
J. Phys. Chem. A 2016, 120, 8949−8969

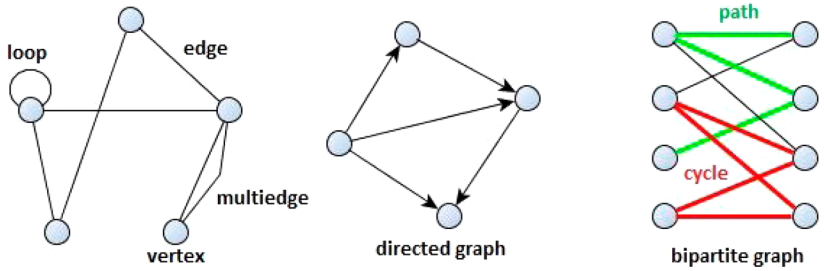

Figure 4. Elementary definitions of graph theory useful to understand characteristics of spectroscopic networks.

account of the structure of SNs and how network theory can be used to better understand high-resolution spectroscopic results. Section 4 summarizes details about the presently most important application of SNs, the MARVEL (Measured Active Rotational−Vibrational Energy Levels) procedure,[48−50] used to determine experimental-quality energy levels from all the available experimentally measured transitions. Section 5 summarizes and concludes our presentation.

2. GRAPH-THEORETICAL FUNDAMENTALS

Though some of the terms utilized are only defined later, we start the discussion with Figure 3, showing the connection between a measured high-resolution spectrum and its spectroscopic network in a simple, pictorial way.

The simulated spectrum shown in Figure 3 is the pure rotational absorption spectrum of $H_2{}^{16}O$ corresponding to its ground vibrational state. Both the line positions and their intensities are taken from a first-principles exact nuclear-motion computation.[15] Each line in the simulated spectrum is color-coded as follows: lines corresponding to *ortho*-$H_2{}^{16}O$ are indicated with black and blue, whereas those of *para*-$H_2{}^{16}O$ with green and red. For all transitions, the color of the lower half of the line corresponds to the lower state, whereas that of the upper half to the upper state. For the more intense lines a quantum-number assignment of the transition is also given, the numbers provided correspond to the rotational quantum number triad $J\ K_a\ K_c$ (*vide infra*). The transitions are indicated by arrows in the two graphs below the spectrum. There is a one-to-one correspondence between the two graphs containing (colored) energy levels and the spectrum containing (colored) transitions. The transitions are represented in the graphs as arrows, because in an absorption spectrum there is always a lower and an upper state and the arrows point from the lower to the upper state. Note that spectroscopic networks will be treated later as undirected graphs. As it is very clear from the two graphs, both for *ortho*- and *para*-$H_2{}^{16}O$ the transitions always connect states where the K_c values have different parity (odd vs even). This figure implies right away important facts about the spectrum of $H_2{}^{16}O$: the graph corresponding to the spectrum contains two components (*ortho*- and *para*-$H_2{}^{16}O$) and each component is a bipartite graph (this explains the use of two colors for each component). It is also evident that the graphs have only even-membered cycles, the smallest cycles have four vertices. The spectrum, at about 205 cm^{-1}, also shows an accidental degeneracy of two transitions, explaining the overlapping colors, one belonging to *ortho*- and one to *para*-$H_2{}^{16}O$. The 3 times larger absorption intensity of the *ortho* transitions as compared to the corresponding *para* transitions, due to nuclear spin statistics, is also clearly visible in the figure, for example at about 150 cm^{-1}.

For the purposes of the present discussion, networks,[5,7] and graphs[37,65−67] are considered to be equivalent mathematical constructs. In what follows, in section 2.1, we give selected definitions of graph theory relevant for the study of spectroscopic networks. Some of the elementary definitions are shown graphically in Figure 4 to help those unfamiliar with graph theory. Section 2.2 introduces the most important matrix representations of networks. This is followed by important concepts useful to understand certain characteristics of SNs, including vertex ranking (section 2.3), and later we discuss complexity measures (section 2.4) and clustering techniques (section 2.5).

The most important terms useful to understand this paper are printed in bold in this section. Therefore, it is hoped that this section can serve as a glossary, where readers can turn to if becoming uncertain about the meaning of a particular term in the later parts of the paper.

2.1. Definitions. Intuitively, a **graph** is a representation of a set of objects where certain pairs of the objects (vertices) are connected by links (edges). Mathematically, a graph G is an ordered pair, $G = (V, E)$, where V is a set of **vertices** and E is a set of **edges**, the edges being two-element subsets of V. If V' is a subset of V, denoted by $V' \subseteq V$, and $E' \subseteq E$, then the graph $G' = (V', E')$ is a **subgraph** of $G = (V, E)$. We will write for the number of vertices $|V| = n$, and for the number of edges $|E| = m$.

Energy levels and transitions among the energy levels of a given quantum system are represented with the vertices and edges of the network G, respectively. An SN of a given molecule "mol" can be denoted as G^{mol}. Further parameters characterizing a spectroscopic network G, *e.g.*, temperature, measurement characteristics (for example, absorption or emission), and a transition intensity cutoff value, can be listed as subscripts to G. Note that the energy levels in an SN carry labels, usually made up of "good" and "approximate" quantum numbers.[44] The labels have to be unique but occasionally it may be advantageous if they not only contain independent but also redundant information.[56,58,59] A further peculiar characteristics of SNs is that the vertices, the rovibronic energy levels, could be ordered on the basis of their energy values (Figure 3). SNs could also be ordered on the basis of quantum numbers; perhaps the most useful quantum number is J, corresponding to the overall rotation of a molecule. This ordering would help placing states connected by strict selection rules close to each other.

The number of transitions (edges) that connect to an energy level (vertex) is called the **degree** of the energy level. Naturally, the sum of the energy level degrees is twice the number of transitions, m. Each edge $e = \{u, v\} \in E$ connects two adjacent vertices $u, v \in V$. If $u = v$, the edge is called a **loop**. SNs do not contain loops. Experimental (measured) SNs are usually **multiedge** graphs, containing multiple edges (between the

DOI: 10.1021/acs.jpca.6b02293
J. Phys. Chem. A 2016, 120, 8949−8969

same pair of vertices), corresponding to multiple measurements of a certain transition. Graphs that contain neither loops nor multiple edges are called **simple graphs**. First-principles SNs, in other words levels and transitions of the computed line list of a molecule corresponding to a chosen measurement technique, are simple graphs. If the edges have no direction, the graph is called **undirected**; otherwise, it is called **directed** (in a directed network the edges have a direction, pointing from one vertex to another). Spectroscopic networks are considered to be and are handled here as undirected graphs though in the case of absorption or emission spectra a direction, based on energy values and leading to a directed graph (Figure 3), could be added.

Sometimes it is useful to assign **weights** to the vertices or edges of the graph. In SNs it is most advantageous to assign non-negative transition intensities to edges as weights. Naturally, other weight choices are also feasible. For example, a positive weight on the vertices of a measured SN can be deduced from the uncertainties of the energy levels, perhaps coming from a MARVEL-type analysis (*vide infra*).

A **path** P of **length** k is a nonempty graph $P = (V_P, E_P)$ of the form $V_P = \{x_0, x_1, ..., x_k\}$ and $E_P = \{x_0x_1, x_1x_2, ..., x_{k-1}x_k\}$, where the x_i are all distinct. An undirected graph G is called **connected** if there is a path between any pair of its vertices. Otherwise, it is called **disconnected**. A **component** S of G is a maximal connected subgraph of G, maximal in the sense that no other vertex (and its edges connecting it to S) can be added to S with preserving the connectedness of S. First-principles SNs are undirected, simple graphs, usually containing more than one component. A component of a graph can have a designated vertex, called the **root**. SNs may contain two types of roots, principal and other. **Principal roots** have a clear physical meaning (note here that the nodes of an SN can be ordered on the basis of their relative energies), as SNs often have two or even three principal roots based on nuclear spin isomerism.[44] The component of an SN containing a principal root is called a **principal component** (PC). A component without a principal root dictated by nuclear-spin isomerism is called a **floating component** (FC). FCs can also have roots but for them this concept does not appear to be useful. A straightforward and fast method for determining the components of a network is the Depth-First Search (DFS) algorithm.[68] A **giant component** is a component whose size is of the same order as $n = |V|$.

The **distance** of two vertices v_1 and v_2 in the same component equals the length of the shortest path between v_1 and v_2, *i.e.*, the path with the smallest number of vertices. The **diameter** of a network is the maximum among the distances between all vertex pairs.

A **cycle** in a graph is a "closed" path: its definition is similar to the definition of the path but with $x_0 = x_k$. SNs contain a large number of cycles of widely differing size. Connected graphs without cycles are called **trees**. A **spanning tree** of a connected graph G is a subgraph T, which is a tree, and contains every vertex from G. A special type of a spanning tree of an edge-weighted graph is the minimum-weight spanning tree: a spanning tree where the sum of the weights on the participating edges is minimal. Regarding SNs, we advocate using the Kruskal algorithm[69] to obtain minimum-weight spanning trees, as SNs are sparse graphs and the Kruskal algorithm handles sparse graphs very efficiently. The implementation of this algorithm is particularly straightforward. For the weight function, the negative logarithm value of the transition intensities on the edges can be used,[53] resulting in a positive and symmetric weight matrix. This way one obtains an **edge-weighted network**, $G^W = (V, E, W)$.

In a **bipartite** graph the vertex set V can be divided into two disjoint subsets V_1 and V_2, with no edges between vertex pairs from the same subset. In other words, for every edge in the graph, one of the end points of the edge is in V_1 and the other is in V_2. If the graph can be colored with two colors, where no edge has the two same-colored end points, then it is bipartite; if an edge violates this coloring, then it is a proof that the graph is not bipartite. The coloring algorithm is best used with an adjacency list data format.

For undirected simple graphs the **edge density** is defined as $D = \frac{2m}{n(n-1)}$. Although in simple graphs the maximum number of edges is $n(n-1)/2$, in SNs this number is much smaller due to the existence of quantum mechanical selection rules, limiting the number of transitions tremendously.[70]

2.2. Matrix Representations of SNs. Matrices provide useful representations for the characterization of SNs.[54] Most notable among these matrices are the **adjacency matrix A**, the **combinatorial Laplacian matrix $\mathbf{L}^C$** (also called the **Kirchhoff matrix**, as it was Kirchhoff who introduced it[71]), and the **normalized Laplacian matrix $\mathbf{L}^N$**. All of these matrices are of size $n \times n$. If we index the vertices as $V = \{v_1, ..., v_i, ..., v_n\}$, then the ith row and column correspond to v_i. Let d_i denote the degree of vertex v_i. Then, the elements of the matrices mentioned are as follows:

$$A_{ij} = \begin{cases} 1, \text{ if there is an edge between } v_i \text{ and } v_j \\ 0, \text{ otherwise} \end{cases} \quad (1)$$

$$L^C_{ij} = \begin{cases} d_i, \text{ if } i = j \\ -1, \text{ if there is an edge between } v_i \text{ and } v_j \\ 0, \text{ otherwise} \end{cases} \quad (2)$$

$$L^N_{ij} = \begin{cases} 1, \text{ if } i = j \\ -(d_i d_j)^{-1/2}, \text{ if there is an edge between } v_i \text{ and } v_j \\ 0, \text{ otherwise} \end{cases} \quad (3)$$

Briefly, the adjacency matrix is used when the network study is aimed at adjacency relations, paths, and cycles. If the SN is undirected and it is without loops and multiedges, **A** is real and symmetric, with real eigenvalues and orthogonal eigenvectors. The symmetric combinatorial Laplacian matrix is a useful tool for dealing with the incidence relations of the edges and vertices and in the matrix tree theorem.[72] Both Laplacian matrices are popular for vertex clustering methods.[73,74] See section 3.9 for some of the uses of **A**, $\mathbf{L}^C$, and $\mathbf{L}^N$ in the case of SNs.

Finally, in ref 54 we introduced the **Ritz-matrix** of spectroscopy, to honor the contributions of Walther Ritz to the field. The Ritz-matrix **X** of a SN is of size $n \times m$, and it is similar to the incidence matrix of a graph in the directed sense:

$$X_{ij} = \begin{cases} +1, \text{ if i is the upper energy level of transition } e_j \\ -1, \text{ if i is the lower energy level of transition } e_j \\ 0, \text{ otherwise} \end{cases} \quad (4)$$

DOI: 10.1021/acs.jpca.6b02293
J. Phys. Chem. A 2016, 120, 8949−8969

The Ritz-matrix plays a vital role in the X-matrix technique introduced by Flaud et al.,[75] forming the basis of the MARVEL procedure,[48−50] at present the principal application based on the idea of SNs (section 4).

2.3. Vertex Ranking. The simplest approach to quantify the importance, called "centrality" in some applications of network theory,[7] of vertices within a set V of an SN is to use the degree distribution. In this case, the most important node will be the energy level with the largest number of associated transitions, the second with the second largest degree, and so on. See sections 3.3 and 3.4 for the degree distributions of experimental and first-principles SNs.

A complementary approach, employed successfully in search optimization engines, is the use of the **PageRank**,[76] a network-based diffusion algorithm.[77] A central feature of this algorithm is that importance depends not only on the number of incoming links but also on the "quality" of the links: a link coming from an important node is much more valuable than a link from an insignificant one. In SNs, this translates to the requirement that regarding the relative importance of an energy level a link to an important energy level, itself having a large number of transitions, is much more important than a link to a marginal one.[54]

The recursive form of the PageRank determination is as follows:

$$PR(i) = \frac{1-\alpha}{n} + \alpha \sum_{j \in M(i)} \frac{PR(j)}{d_j} \tag{5}$$

where $PR(i)$ is the PageRank of the ith node, $M(i)$ is the set of neighbors of the ith node, and $\alpha \in (0, 1)$ is a dampening factor. It is important to note that if we take an ordering of the vertices based on their PageRank value, changing α does not alter the order. Because we do not intend to use the numerical PageRank values, our aim is simply to use them for the ranking itself, we can take an arbitrary α, for example, $\alpha = 0.5$. See section 3.6 for related results for SNs.

2.4. Complexity Measures. There are several metrics developed to describe the complexity of a network. The most notable of them are the local clustering coefficient, $C(G)$, the structural metric (or s-metric) with the corresponding $S(G)$ value, and the Pearson correlation coefficient, $r(G)$,[78] which is a graph assortativity measure.

The **local clustering coefficient** gives information on how close the investigated graph is to the complete graph. More specifically, it quantifies every vertex on a [0, 1] scale and shows how close the vertex is to form a clique (a complete graph) with its neighbors. Because SNs cannot have cliques and cannot have odd-numbered cycles, this measure is not particularly useful for the understanding of the structure of SNs.

The **structural metric** (s-metric) is defined as

$$s = \sum_{i,j \in V} d_i d_j \tag{6}$$

where d_i is the degree of node i. If we introduce s_{max} as

$$s_{max} = \sum_{i=1}^{n} \frac{{d_i}^3}{2} \tag{7}$$

we can define the normalized structural metric, $S(G)$, as

$$S(G) = \frac{s}{s_{max}} \tag{8}$$

The **Pearson correlation coefficient** of the degrees at either end of an edge is defined as

$$r(G) = \frac{\sum_{i,j \in T} \frac{d_i d_j}{l} - \left(\sum_{i,j \in T} \frac{d_i + d_j}{2l}\right)^2}{\sum_{i,j \in T} \frac{{d_i}^2 + {d_j}^2}{2l} - \left(\sum_{i,j \in T} \frac{d_i + d_j}{2l}\right)^2} \tag{9}$$

where l is the number of edges in the graph. $r(G)$ has been introduced to analyze the assortativity of a network. Social networks, for example, usually show **assortativity mixing** on their degrees;[7,78] that is, their high-degree vertices like to connect to other high-degree vertices in the network. The opposite of assortativity mixing is **disassortativity mixing**, whereby high-degree vertices attach to low-degree ones. The latter property is frequent in technological and biological networks.[7,78]

2.5. Vertex Clustering. The principal aim of vertex clustering is to distribute the vertices of a network into clusters along predefined properties.[73] The subsets the partitioning yields must be pairwise disjoint, and their union should be the original vertex set. If we distribute a partition into k subsets, we call it a **k-clustering**.

Clustering algorithms can be divided into at least two classes: partition and hierarchical clustering.[79] Partition clustering methods generate a starting partition first, then re-evaluate the actual clustering in each step in an iterative loop until arrive at the required clustering result. Hierarchical clustering algorithms are using the iteration of either merging smaller clusters to larger ones (in **agglomerative clustering**), or dividing larger clusters into smaller ones (in **divisive clustering**), based on a similarity measure. Both types of clustering result in a hierarchy of clusters, called a **dendogram**. Generally, partition clustering techniques are faster, but they require more information beforehand (for example, the number of clusters in the network). The Clauset−Newman−Moore (CNM) algorithm[80] is an efficient hierarchical agglomerative algorithm that can be used for clustering of even large networks, like SNs. It is useful for highlighting communities within a network. One can use the Stanford Network Analysis Platform (SNAP)[81] for CNM clustering. Maintaining a balance in the size of the subsets during the clustering is definitely a preferred property. Normalization means that the clusters obtained should have roughly the same size.

Spectral clustering algorithms[73] are applicable for partition clustering. To determine a partitioning of the energy levels of one of the PCs of an experimental SN, the spectral clustering technique utilizes the eigenvalue spectra of $\mathbf{L}^C$ or $\mathbf{L}^N$.

One can calculate a k-clustering of a network using the eigenspectra of the normalized Laplacian matrix, $\mathbf{L}^N$, of the network. It is especially meaningful in spectroscopy to look for a partitioning where the number of edges is minimal between the different clusters. This way one forms "communities" within the network: a community G' is defined when the sum of all degrees of vertices within G' is (much) larger than the sum of all degrees toward the rest of the network. To obtain a k-clustering of this type, one should determine k eigenvectors corresponding to the largest eigenvalues of $\mathbf{L}^N$, form a matrix of size $n \times k$ where the eigenvectors are in the columns, normalize the rows, and then apply a k-means clustering to the rows, which are considered to be n k-dimensional points.

Another useful concept that can be employed in high-resolution molecular spectroscopy is that of the **bridge**. A

DOI: 10.1021/acs.jpca.6b02293
J. Phys. Chem. A 2016, 120, 8949−8969

bridge is an edge of a network whose deletion increases the number of connected components. Naturally, a bridge may not be a member of any cycle. One of the simplest (and fastest) bridge-finding techniques[82] uses the DFS algorithm.[68] Finding bridges in SNs is useful because (a) exploring connectors of larger subgraphs can help to explore the weakly connected components of the SN (if an energy level is a member of a weakly connected cluster, then its uncertainty highly depends on the accuracy of the bridge) and (b) exploring branches (Figure 9, *vide infra*) helps to detect those energy levels whose values are the least reliable.

3. STRUCTURE OF SPECTROSCOPIC NETWORKS

Based on the network definitions and concepts presented in section 2, the questions raised toward the end of the Introduction can be answered and a number of useful statements can be developed about different aspects of the structure of SNs. These statements contribute to our improved understanding of the results of high-resolution molecular spectroscopic experiments as well as of data deposited in spectroscopic information systems.

For some of the structural properties it is important to distinguish between experimental and first-principles SNs of a molecule. Construction of an experimental SN is obvious: one needs to collect all assigned transitions from the literature (see Table 1 for the number of sources identified during the building of SNs for the molecules studied thus far). Construction of a first-principles SN goes through the following steps: (a) take all (available) computed energy levels as nodes; (b) use the selection rules appropriate for the molecule and the experiment to link the nodes; and (c) add the computed intensities, serving as network weights, as well, to the links based on the type of experiment and the chosen temperature. Transition intensity cutoff values can be used to select a subset of the possible links, as done in the panels of Figure 2. In this section we usually concentrate on experimental SNs, whereas first-principles ones receive somewhat less attention.

So far, the experimental SNs of 15 molecules have been investigated. The list of molecules include nine isotopologues of water,[40−43] three isotopologues of H_3^+,[56,57] and $^{12}C_2$,[59] $^{14}NH_3$,[58,83] and ketene, $^{12}CH_2{}^{12}C^{16}O$.[55] Table 1 lists some of the principal characteristics of the experimental SNs of these molecules. Table 2 lists data relevant for spectroscopic networks contained in the canonical line-by-line information system HITRAN[24,25] and investigated in this study. The HITRAN database contains not only experimental data but also accurate computed ones when available and needed. A note about the HITRAN data used in this study: among the large number of transitions present in HITRAN for a large number of molecules, there are some that seemingly correspond to forbidden transitions. For example, the HITRAN data for $H_2{}^{16}O$ contain five transitions that violate the *ortho*−*para* selection rule. The frequencies of these transitions are 11069.73629, 19430.03950, 19706.8374, 19870.5948, and 21295.3901 cm^{-1}. These transitions were removed from the present analysis. Another example is the H_2O_2 molecule, where the HITRAN data lead to the presence of a three-membered cycle. This odd-membered cycle violates the one-photon selection rules and the bipartiteness of the corresponding SN (subsection 3.2, *vide infra*); therefore, these transitions, at 18.975258, 1387.383507, and 1393.928115 cm^{-1}, were also removed before our analysis. Most of the discussion within this section focuses on data in Tables 1 and 2.

Table 2. Selected data about spectroscopic networks found in the canonical spectroscopic database HITRAN.[25]

HITRAN index	name	no. of nodes	no. of unique links	no. of components	bipartite
1	water	17045	134063	2	true
3	ozone	38816	260094	24	true
9	sulfur dioxide	18054	72460	1	true
10	nitrogen dioxide	6931	26334	5	true
20	formaldehyde	9847	40670	14	true
25	hydrogen peroxide	14975	126949	24	true
32	formic acid	11385	62684	1	true

3.1. Components of SNs.

First-principles complete SNs of molecules may have several principal components (PCs, not to be confused with the unrelated principal components analysis), as required by nuclear spin statistics.[44] Each PC has a root, which can conveniently be chosen as the lowest-energy level of the PC. PCs are expected to be giant components of SNs. Selection rules put constraints on the changes of the ("good" and "approximate") quantum numbers describing the energy levels involved in the transitions within a SN. Under field-free conditions, transitions are not allowed among the energy levels belonging to different PCs.[84] Therefore, it is challenging to measure the energy difference between the roots of the PCs (*vide infra*).

As an example, we note that symmetric isotopologues of water (*e.g.*, $H_2{}^{16}O$, $H_2{}^{17}O$, $H_2{}^{18}O$, or the similar three isotopologues of D_2O) have two principal components, traditionally[44] called *ortho* and *para* [depending on whether the spins of the protons are parallel (*ortho*, total nuclear spin I = 1) or antiparallel (*para*, I = 0)]. On the contrary, the SN of the $HD^{16}O$ isotopologue of water, with all of its nuclei different, has only a single PC; *i.e.*, all of the energy levels of $HD^{16}O$ form part of the same first-principles SN.

Figure 5 shows the lowest-energy part of the complete purely rotational one-photon absorption SN of the $HD^{16}O$ molecule, up to J = 3, where J is the rotational quantum number and K_a and K_c are the usual asymmetric-top quantum numbers.[44,85] The selection rules behind the connectivity of the energy levels state that if $\Delta J = 0(\pm 1)$ then $p = \pm 1(0)$, where p is the parity describing the energy level. These rules dictate that if the rotational parity, defined as $(-1)^{K_c}$, is even or odd, then the maximum number of pure rotational transitions from a given rovibrational energy level with asymmetric-top label[85] $J_{K_aK_c}$ is $3J$ + 2 or $3J$ + 1, respectively, as shown in Figure 4. It is important to observe that not all rotational transitions emanating from even the lowest-J states have been measured, though the $HD^{16}O$ molecule is thoroughly studied experimentally; see ref 41 and the data in Table 1. As J increases, the number of transitions not measured increases rapidly (not shown in Figure 5). Note that although many of the transitions may not be measured directly, their absence does not hinder obtaining the complete tree structure of the SN. Furthermore, identification of the missing transitions in experimental spectra becomes straightforward if the "inverted" rovibrational energies are available and the transition intensity, perhaps computed *ab initio*, is sufficiently large.[55] Note also the apparent lack of odd-numbered cycles in Figure 5.

DOI: 10.1021/acs.jpca.6b02293
J. Phys. Chem. A 2016, 120, 8949−8969

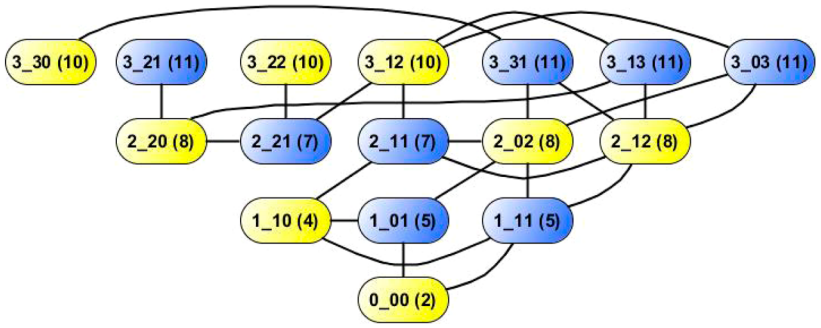

Figure 5. Experimental purely rotational one-photon absorption spectroscopic network of $HD^{16}O$ in the ground vibrational state up to $J = 3$ (the root of the graph is the $J_{K_aK_c} = 0_{00}$ state, the notation is changed in the figure to $J\_K_aK_c$). The number in parentheses in each oval, representing an energy level, provides the number of allowed rotational transitions starting or ending on the given energy level within the ground vibrational state. The bipartite nature of the network is indicated with the two different background colors of the energy levels. The nodes (energy levels) are connected if the transition has been measured experimentally.

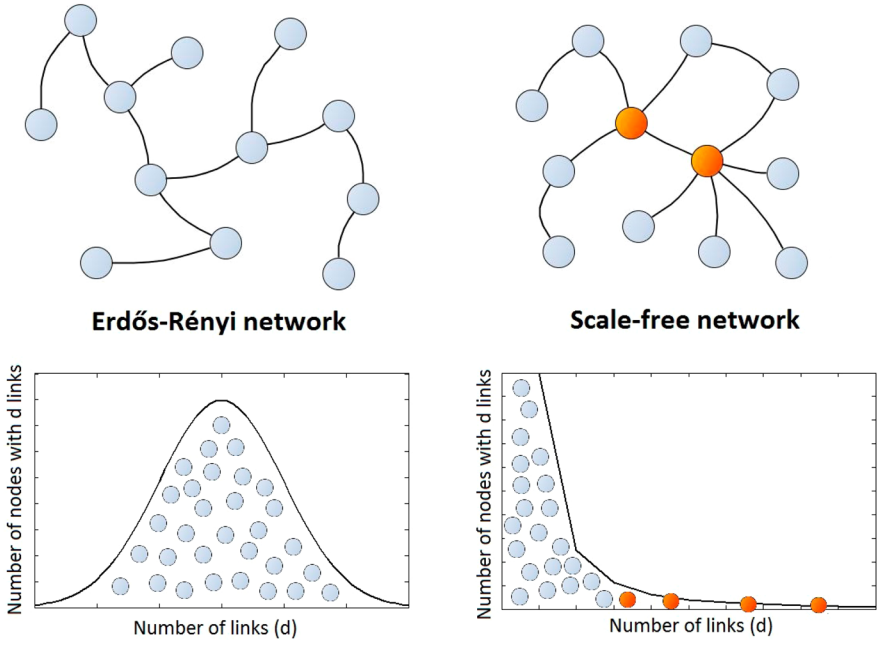

Figure 6. Pictorial representations and degree distributions of random networks of Erdős–Rényi (left panels) and of scale-free (right panels) character, the so-called hubs (nodes with a large number of links) are shown in orange in the latter case.

Experimental SNs form multiedge graphs. As measurements done by different groups use different techniques and spectrometers working in different regions of the electromagnetic spectrum, there is some randomness in how transitions become measured. Thus, in principle spectroscopic measurements could result in several components. We did not find a case[40−59] where the experimental SN of a molecule contained a large number of FCs, in all cases the great majority of the energy levels and transitions were part of the PCs of the network.

The size of a first-principles SN, both in the number of nodes and especially in the number of links, depends heavily on the chosen transition intensity cutoff. We did not find a case where first-principles SNs contained, at whatever intensity cutoff value, floating components, the transitions selected this way always belonged to the PCs. Thus, both the experimental and the first-principles SNs seem to have giant components, an observation that can be explained by the degree distribution of SNs (see subsections 3.3 and 3.4).

Attempts to unite the components of an experimental SN are important for several reasons, most importantly as they (a) allow the attachment of proper, "absolute" energy values to the vertices of the components disjoint from the PCs having the energy zero; (b) help to improve the robustness of the SN; and (c) may lead to the design of new experiments and/or suggest to study certain spectral regions to improve the information content of the SN.

As shown in ref 54, even for the smallest experimental SNs studied there is an extremely large number of possible spanning trees for each of the PCs, on the order of 10^{10}–10^{50}. Nevertheless, because a unique weight can be assigned to each link (a unique transition intensity in the cases studied), there will be a unique minimum-weight spanning tree for each component. Investigation and comparison of the structure of the experimental and first-principles minimum-weight spanning forests provides the simplest and most efficient way to connect the possible FCs to PCs, the giant components of the SN.

Finally, there is another statement that the investigation of the structure of first-principles SNs of different size yields:

DOI: 10.1021/acs.jpca.6b02293
J. Phys. Chem. A 2016, 120, 8949−8969

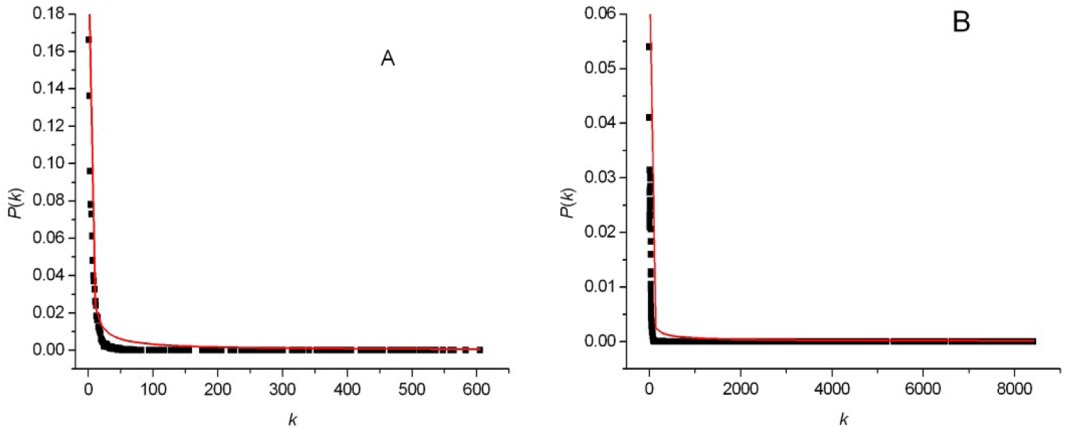

Figure 7. Size–frequency [k–$P(k)$] plots for measured (panel A) and first-principles computed (panel B) transitions for $HD^{16}O$, with an absorption intensity cutoff of 10^{-22} cm molecule^{-1} in the latter case.

Table 3. Power-Law Distribution Fittings to the Principal Components (pc) of the Spectroscopic Networks of Selected Molecules Present in the HITRAN Information System[a]

HITRAN index	name	no. of nodes	no. of links	γ	x_{min}	x_{max}	$KS.p$	avg degree	diam	avg dist
1	water pc#1	7871	59560	2.01	150	805	0.39	15.1	27	5.8
1	water pc#2	9174	74503	2.05	180	879	0.27	16.2	28	6.0
3	ozone	38719	260006	2.26	667	5666	0.95	13.4	88	20.0
9	sulfur dioxide	18054	72460	1.99	54	5919	0.87	8.0	101	25.8
10	nitrogen dioxide	6778	26086	1.76	31	1870	0.99	7.7	103	22.4
20	formaldehyde pc#1	5007	21656	2.18	200	795	0.41	8.7	65	13.7
20	formaldehyde pc#2	4610	18796	2.84	300	856	0.33	8.2	62	13.7
25	hydrogen peroxide pc#1	7604	69160	2.23	51	469	0.87	18.2	50	14.2
25	hydrogen peroxide pc#2	7213	57650	2.52	86	723	1.00	16.0	50	14.3
32	formic acid	11385	62684	2.15	200	1610	0.38	11.0	81	22.9

[a]PC = principal component, diameter = diameter, avg = average, dist = distance. See the text for further definitions employed in the table.

although the great majority of the transitions is extremely weak, it is easy to find a few relatively strong transitions for almost all vertices in the SN. This suggests that with relatively standard spectroscopic measurements almost all of the energy levels can be determined, which in turn could lead to an almost complete knowledge of high-resolution experimental absorption (and emission) spectra if transitions based on "measured" energy levels were augmented with computed line intensity values.

3.2. Bipartiteness. There is a highly special and highly restrictive property of SNs related to the quantum mechanical selection rules: all the SNs investigated thus far (see the entries of Tables 1 and 2 for the list of molecules) are bipartite networks. This reflects an important property of rovibrational states, namely their overall parity, which has to change during experimentally measurable one-photon transitions. A corollary of bipartiteness, important for all spectroscopists and users of spectroscopic information, is the fact that, as long as the parity selection rule of molecular rovibrational transitions is not violated, there are no simple cycles of odd length in SNs, the smallest cycle must involve four energy levels and there are only even-numbered cycles in SNs.

As shown in Table 2, all the SNs selected from the canonical spectroscopic database, HITRAN,[25] are bipartite. This suggests that the spectroscopic data in HITRAN are correct for these molecules, at least in this sense.

3.3. Degree Distribution of SNs. In network theory a network G with n vertices and m edges is said to be *sparse* if $m \ll n^2$ and *dense* if $m = O(n^2)$. Clearly, all experimental and first-principles SNs are sparse networks.

Erdős–Rényi random graphs[34−36] are built by a process whereby links are placed randomly between a fixed number of vertices. Erdős–Rényi random graphs with a fixed set of V_{fix} vertices have a "characteristic" degree $2E/V_{fix}$; *i.e.*, the vertex degrees have approximately a Poisson distribution with a mean of $2E/V_{fix}$ (Figure 6). If a random graph is allowed to grow and links are added on the basis of probabilities proportional to the momentary degrees of the vertices, a scale-free (SF) random graph results.[7] The scale-free property of a network means that the probability that a randomly selected node has exactly d links is $P(d) \propto d^{-\gamma}$, where γ is called the *scaling index*.[5] SF random networks, as opposed to Erdős–Rényi random networks, are characterized by (a) a relatively few nodes with a large number of links (these nodes are called *hubs*), and (b) a robust connectivity structure hard to fragment by random removal of nodes. The following dynamical features are the usually assumed requirements of a SF random network:[7] (a) evolutionary growth with more or less random generation of new nodes, (b) highly interactive self-organization, and (c) preferential connectivity of new nodes to old ones. Hubs shorten the paths between vertices of a network.

Features of SF networks mentioned occur naturally for SNs on the basis of spectroscopic experiments. For complete first-principles SNs this is not true; nevertheless, if the intensities of the transitions, always spanning many orders of magnitude, are taken into account, first-principles SNs also become scale free. Naturally, the size of a first-principles SN, in the number of both energy levels (nodes) and transitions (links), depends on the chosen cutoff of the absorption intensities. The computed

DOI: 10.1021/acs.jpca.6b02293
J. Phys. Chem. A 2016, 120, 8949−8969

SN of $HD^{16}O$ contains[16] altogether 163491 energy levels and 697444828 transitions. At 298 K, if the absorption intensity cutoff is chosen to be 10^{-20} cm molecule^{-1}, the SN contains 73590 nodes and 863575 links. With still realistic cutoffs of 10^{-24} and 10^{-28} cm molecule^{-1}, the first-principles SN of $HD^{16}O$ contains 128106 (4720711) and 153600 (15356682) nodes (links), respectively. From the numbers presented it is clear that the number of energy levels grows much more slowly than the number of transitions, the great majority of the transitions is extremely weak. All these SNs are characterized by a SF distribution; see two representative examples in Figure 7.

The degree distributions of the molecules selected from the HITRAN database, Table 3, also exhibit heavy tails. The γ column of Table 3 contains scaling indices for 10 principal components. The x_{min} values are the lower bounds for the vertex degree frequencies considered during the fitting. *KS.p* is the *p*-value of the Kolmogorov−Smirnov test with the corresponding γ and x_{min} parameters. The x_{max} parameter denotes the highest among the degree frequencies in the component. It seems that for most molecular species, if not for all, the degree distribution is scale-free. Some of the most important consequences of this observation are discussed in section 3.5. Furthermore, the scaling indices are all larger than 2.0; their average value is about 2.2.

3.4. First- and Second-Degree Distributions. There is no established spectroscopic law requiring that the most intense lines, those that can be most easily measured, should form a connected component. Nevertheless, Figures 1 and 2 clearly show that there is only one large connected component for either the *ortho* or the *para* principal components of the SN of $H_2^{16}O$, independently of the time of the measurements collected or the line intensity cutoff value chosen. A network component whose size grows in proportion to number of nodes is called[7] a *giant component*. Thus, our observations tell us that SNs have giant components. It is worth investigating modeling efforts that could rationalize this observation.

The *n*th moment of $P(d)$ is defined as

$$\langle d^n \rangle = \sum d^n P(d) \tag{10}$$

The first moment, $\langle d \rangle$, is called the *mean vertex degree* of *G*. The mean vertex degree remains finite as long as $\gamma > 2$, which appears to be true for the SNs studied. The second moment, $\langle d^2 \rangle$, is the *mean number of second neighbors* and measures, as usual, the fluctuations of the connectivity distribution. Using the first and second moments, the following condition can be written for the existence of a giant component:[86]

$$\langle d^2 \rangle - 2\langle d \rangle > 0 \tag{11}$$

As the data in Table 4 clearly suggest for the three largest experimental SNs,[42,58,59] these SNs must have a giant component.

There is another condition that can be used when the existence of a giant component is investigated. The average number of second neighbors is

$$c_2 = \langle d^2 \rangle - \langle d \rangle$$

so a giant component exists if

$$c_2 > \langle d \rangle$$

Furthermore, knowing the average number of the first and second neighbors, an interesting relation can be given for the mean number of neighbors at any distance *d*,

Table 4. First and Second Moments, and the Mean Number of the Second and Third Neighbors, in the Experimental Spectroscopic Networks of Selected Small Molecules

molecule	ref	$\langle d \rangle$	$\langle d^2 \rangle$	c_2	c_3
o-$H_2^{16}O$	42	11.89	839.26	827.37	57572.8
p-$H_2^{16}O$	42	9.05	633.07	624.02	43027.7
o-NH_3	58	11.50	683.71	672.21	39292.7
p-NH_3	58	11.05	629.94	618.89	34662.7
$^{12}C_2$	59	6.16	69.87	63.71	659.1

$$c_d = \left(\frac{c_2}{c_1}\right)^{d-1} c_1 \tag{12}$$

For comparative purposes, Table 4 contains the values of c_3 obtained this way.

Modeling studies[87] employing "pure" power-law degree distributions provide interesting results about the size of the largest components, associated for SNs with PCs. The most relevant statements are as follows: (a) a network will have a giant component if $\gamma < 3.4788...$ but not if it is larger; (b) the giant component corresponds to the entire network when $\gamma \leq 2$; and (c) in the region between $\gamma = 2$ and $\gamma = 3.4788...$ there is a giant component but it does not fill the whole network. Because experimental SNs seem to have $\gamma \approx 2.2$, Table 2, these modeling studies nicely support the observation that experimental SNs have giant components and occasionally some small ones. Nevertheless, note that first-principles SNs obtained with reasonable intensity cutoff criteria seem to have only giant components.

The degree distribution completely determines the statistical properties of uncorrelated networks. As the related investigations show,[7] a large number of real networks are *correlated*, meaning that the probability that a node of degree *k* connects to a node of degree *k*′ depends on *k*.

3.5. Hubs and Edge Densities. Scale-free networks contain a small number of hubs. As expected, the hubs with the largest number of degrees in a one-photon absorption SN are on the ground vibrational state. For the measured SN[41] of $G^{HD^{16}O}$ they are as follows: $J_{K_aK_c} = 4_{22}$, 4_{23}, and 3_{13}, with 605, 583, and 565 links, respectively. In the computed SN, with a cutoff value of 10^{-30} cm molecule^{-1}, the nodes with the largest number of connections are $6_{34}(4042)$, $7_{35}(3970)$, and $6_{24}(3897)$, where the number of links is given in parentheses.

The scale-free property of SNs means that despite the fact that SNs can be extremely large (though always finite in realistic cases), there are only relatively few energy levels whose accuracy principally determines the overall accuracy of the energy levels of an experimental SN. Experiments which improve the accuracy of SNs by decreasing the uncertainties of energy levels qualifying to be hubs are the most useful ones. This leads to the important conclusion that all microwave (MW), millimeter wave (MMW), and far-infrared (FIR) measurements performed with this aim in mind would be highly beneficial for improving the overall accuracy of experimental SNs of small molecules of prime interest for sophisticated modeling studies.

For undirected simple graphs, like the SNs, the edge density is defined as $D = 2|E|/[|V|(|V| - 1)]$. Although in simple graphs the maximum number of edges is $|V|(|V| - 1)/2$, in SNs this is much smaller due to the constraints provided by the quantum mechanical selection rules. As shown in Table 1 of ref 52, the

DOI: 10.1021/acs.jpca.6b02293
J. Phys. Chem. A 2016, 120, 8949−8969

edge density D of the first-principles SNs of $HD^{16}O$, with intensity cutoff values ranging from 10^{-20} to 10^{-90} cm molecule^{-1}, has a minimum at about 10^{-30} cm molecule^{-1}. This minimum is achieved at an intensity value that is about the limit for present-day absorption measurements. Nevertheless, it must not be forgotten that the investigated line list becomes incomplete at about this intensity cutoff value.

As shown in ref 53, the behavior of hubs within the SN can be described using graph metrics (section 2.4). For the first-principles model of the $H_2{}^{16}O$ molecule with an intensity cutoff 10^{-20} cm molecule^{-1}, we have an $r(G)$ value that is close to zero, with a relatively large $S(G)$. This translates to the fact that hubs like to connect to each other in the spectroscopic network, although the hubs also have many low-degree neighbors. Moreover, as we reduce the absorption intensity cutoff parameter (to 10^{-22}, 10^{-24}, 10^{-26}, and 10^{-28} cm molecule^{-1}), it becomes obvious that the SN becomes increasingly disassortative, as many new transitions appear with low-degree nodes at one or both end points. This in turn lowers the ratio of the edges which connect two high-degree nodes in the SN.

3.6. PageRank. Determining a useful importance ordering ("centrality measure") for the set of energy levels of a SN is important for orienting high-resolution spectroscopists and spectroscopic information system developers, as well. Importance is an intuitive term here, but it refers to various enquiries, including (1) which energy levels have the largest number of transitions associated with them, (2) which energy levels are present in the largest number of cycles in the SN, or (3) which energy levels are affecting the uncertainties and their propagation in the SN the most.

Question 1, for example, can be answered by setting up the **A** matrix, as the degree d_i of vertex i of G, *i.e.*, the number of its connections, is simply $d_i = \Sigma_{j=1}^{n} A_{ij}$. Note that the degree of an energy level may not reflect properly the importance of even a hub, as most connections may be made to low-degree energy levels. Answering question 2 is a difficult and computationally demanding task, especially because SNs have a very large number of cycles of very different size (see Figure 3 for a simple case). Nevertheless, answering the question whether the energy level is part of even one cycle, which should significantly help its accurate determination, is straightforward. The answer to question 3 will be discussed in some more detail in the subsection on network clustering.

The PageRank order of the hubs can be significantly different from their degree order. PageRank ordering appears to be a more useful measure to judge the relative importance of the most important energy levels (hubs) as within the PageRank ordering hubs are preferentially connected with hubs. For $H_2{}^{16}O$, for example, the most important hubs with the highest degrees and the highest PageRanks are all on the vibrational ground state and have J values around 5.

An example to demonstrate the usefulness of the PageRank ordering was given in ref 54 during the investigation of the SN of *ortho*-H_3^+. We omit the explanation of the labels of the energy levels investigated, we refer the interested reader to ref 56. The maximum vertex degree in the SN of *o*-H_3^+ is 28; therefore, the energy level (0 0 0 1 0 m) with a degree of 22 would be considered important based purely on the degree ordering. However, 14 of the 22 transitions of this node are connected to 1-degree nodes (leaves), which are not significant in the SN. The maximum PageRank value belongs to the energy level (0 1 1 4 3 u), with a vertex degree of only 9. Nevertheless, every neighbor is present in at least one cycle, and the vertex with the maximum degree in the SN is also among the neighbors. Thus, we must consider the latter energy level more important in this SN than the former one.

Furthermore, Figure 8 compares the structure of the 10 most central energy levels in the SN of *o*-H_3^+ with respect to degree ordering (left panel) and PageRank ordering (right panel). Notice that only four nodes, those colored green in the figure, are present in both lists. Moreover, the subgraph defined by the ten nodes having the highest degrees is disconnected, in other words, these nodes do not form one connected component, instead, they form six. When PageRank defines the centrality, the subgraph is well connected with a lot of cycles, with an eminent participation of hubs in these cycles. As cycles are especially important in validating measurements, we must consider the use of the PageRank ordering advantageous.

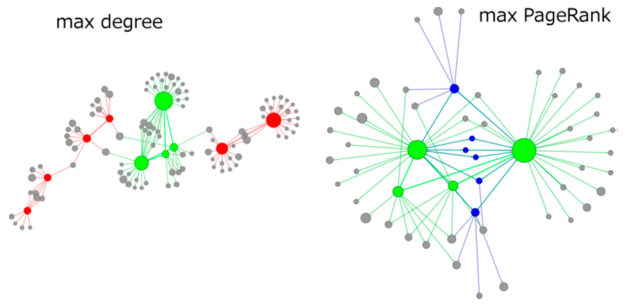

Figure 8. Top 10 most important nodes in the SN of *ortho*-H_3^+ based on vertex degree ordering (left panel) and PageRank ordering (right panel). Green: nodes in both top 10 lists. Red: nodes only among the top 10 degree values. Blue: nodes only among the top 10 PageRank values.

3.7. Diameter. There are additional signatures beyond the power-law degree distribution that characterize SF networks. An important one is the small-world property: scale-free networks are characterized by a small diameter.

The diameter of a network is defined as the maximum distance of a vertex pair; in other words, the longest path of the shortest paths among all vertex pairs. The diameter of the SN can be estimated by counting the different eigenvalues of **A**: if **A** has r different eigenvalues, then the diameter of G is at most $r - 1$.

The interconnectedness of a particular SN can be described efficiently by the diameter. The diameter computed statistically for the measured SN of $HD^{16}O$ is only about 7, though it is still considerably larger than the corresponding log ν value, about 3. This value is slightly larger but similar to the diameter of the first-principles SN. As the absorption intensity cutoff is decreased, the diameter of the computed SN seems to stay around this value though it becomes somewhat smaller. Thus, SNs clearly have an intrinsic small-world property, similarly to most other complex networks studied in nature, society, communication, and elsewhere.[7,11,88]

3.8. Network Vulnerability. Selection rules allow only a limited number of links between the nodes of the SN. As the SN becomes larger, either via new measurements for an experimental SN or by a decrease in the intensity cutoff for a first-principles SN, the number of links increases substantially but not the number of nodes. The number of (even-membered) cycles within the network also increases dramat-

DOI: 10.1021/acs.jpca.6b02293
J. Phys. Chem. A 2016, 120, 8949−8969

ically. This is in full accord with the degree distribution observed for SNs. Thus, SNs appear to be robust.

Robustness of SNs can be ascertained by a numerical experiment involving random removal of nodes.[8,52] The results for three selected SNs corresponding to $HD^{16}O$, one being the measured SN, the other a first-principles SN, and the third the purely rotational first-principles SN, are shown in Figure 9.

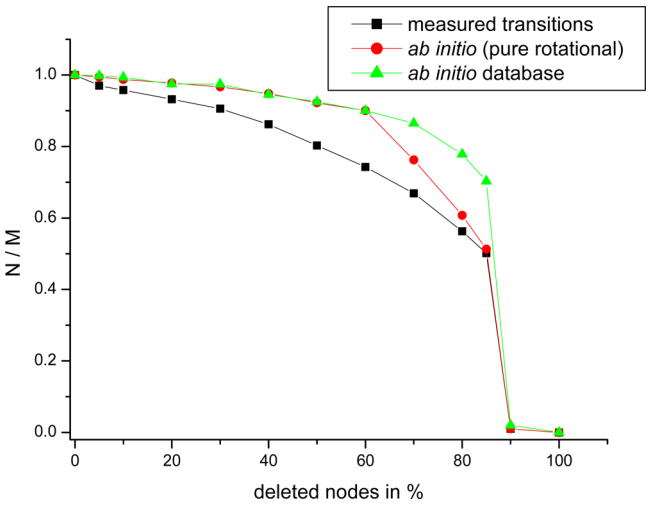

Figure 9. Fragmentation dynamics of spectroscopic networks following random removal of nodes, where N/M means the number of nodes within the largest remaining network (N) compared to the maximum number of nodes (M) in the SN.

After random removal of nodes, the relative size of the largest remaining network compared to the full size of the network remains very close to 1 even if up to 70% of the nodes are removed. The network only fragments when about 85% of the nodes are randomly removed. This extreme error tolerance is another characteristic property of SNs.

In SF networks removal of nodes leads to an increase in the diameter;[8] of course, this has also been observed for SNs.[53]

3.9. Matrix Representations of SNs. As detailed in section 2, there are several matrices that can be used to describe different aspects of the structure of spectroscopic networks. The spectra (here eigenspectra) of these matrices reveal several properties of SNs without the need for an explicit analysis of the exact SN structure.[54]

The bipartite character of a network can be detected using the eigenvalues of the adjacency matrix **A**. If the eigenvalue spectrum of **A** is symmetric about the origin, the network is bipartite. If the network is connected, it is sufficient to check that the smallest eigenvalue is the negative of the largest eigenvalue, this ensures bipartiteness of the network. Bipartiteness is also related to the powers of **A**. Let $\mathbf{A}^k$ be the kth power of the adjacency matrix. The ijth element of $\mathbf{A}^k$ is equal to the number of walks of length k, starting from vertex i and ending on vertex j. The fact that there are no simple cycles of odd length in a bipartite graph implies that for odd k powers of **A**, $A_{ii}^k = 0$ holds for the diagonal entries.

If the multiplicity of the zero eigenvalue of the combinatorial Laplacian matrix $\mathbf{L}^C$ is greater than 1, then the network is not connected; *i.e.*, it contains more than one component. In general, the multiplicity of the zero eigenvalue is equal to the number of connected components of the network. The second smallest eigenvalue, λ_2, can be used to give a lower bound to the minimum cut in a network: for $A, B \subseteq V(G)$, $A \cup B = V(G)$, $A \cap B = \varnothing$, and $e(A,B)$ denoting the number of edges with one end point in A, and the other end point in B, it holds that $\lambda_2 \frac{|A||B|}{|V(G)|} \leq e(A,B)$.[89]

The Ritz-matrix **X** can also be called the design matrix, as this is the matrix that can be used to obtain the unknown energy levels from the known transitions via a (weighted) linear least-squares analysis, as done within the MARVEL protocol.[48−50] The relation $\mathbf{X}\mathbf{X}^T = \mathbf{D} + \mathbf{A}$ holds among the matrices useful for investigating SNs, where **D** is the diagonal matrix with the degrees in its diagonal.

The number of nonidentical spanning trees, $\tau(G)$, can be calculated from $\mathbf{L}^C$ using the following formula:

$$\tau(G) = \frac{1}{n}\prod_{i=1}^{n-1}\lambda_i \tag{13}$$

As shown in ref 54, this formula gives extremely large values for the number of spanning trees even for relatively small SNs. Thus, weighting introduced to SNs serves a special purpose if spanning trees are to be used for high-resolution spectroscopy.

3.10. Clustering. Connectors between relatively dense subnetworks (clusters) of SNs can be identified and analyzed via several variants of spectral clustering techniques[73] based on the combinatorial and normalized Laplacian matrices introduced in section 2, $\mathbf{L}^C$ and $\mathbf{L}^N$, respectively.

The partition and hierarchical clustering results appear to have considerable value in identifying the "weakest links", from an information system point of view the most significant links in the SN. Identification of these links is especially important as they may limit the accuracy of the determination of a large number of energy levels, separated from well-defined energy levels by the small number of connectors, even if these energy levels form part of several (local) cycles. The identification of "weakest links" becomes especially important when one judges the true accuracy of the experimental rovibrational energy levels obtained through the MARVEL approach, which converts information in measured transitions to information about the energy levels of a molecule.

The number of bridges in the experimental SNs of $H_2{}^{16}O$, $^{14}NH_3$, and $^{12}C_2$ of the present analysis is 3513, 730, and 1296, respectively. Comparing these values with the total number of links (98838, 15393, and 16481, respectively) suggests that, in a relative sense, it is the database of $^{12}C_2$ that contains the largest number of bridges. This explains why the diameter of the experimental SN of $^{12}C_2$ is much larger than usual (see Table 2 of ref 54). The number of energy levels whose values depend on bridge transitions are 4865, 965, and 1575 for $H_2{}^{16}O$, $^{14}NH_3$, and $^{12}C_2$, respectively. The energy level values might be incorrect because they heavily rely on the correctness and accuracy of a single transitions.

3.11. Data Reduction via SNs. Because high-resolution spectroscopic measurements yield an extreme amount of information, the reduction of the observed data to manageable size is a basic challenge for the theory of spectroscopy. The standard solution is to use model Hamiltonians with a relatively small number of parameters and least-squares optimize these parameters to represent all the measured data.[90] In a way this means that spectroscopic transitions are converted to parameters yielding energy levels (and transitions via the Ritz principle). These parameters allow excellent interpolation but they may fail when used to extrapolate beyond the measured

DOI: 10.1021/acs.jpca.6b02293
J. Phys. Chem. A 2016, 120, 8949−8969

range (especially if one considers the extremely high accuracy of most of the measurements).

SNs offer another, somewhat less spectacular data reduction facility via the inversion of transitions to energy levels. The best way to reduce the information content of experimental transitions is through the use of weighted spanning trees corresponding to the experimental SN. This way one can reduce the information contained in the huge number of measured transitions of the network to a relatively small set of energy levels and transitions (the saving is about an order of magnitude, Table 1, but grows fast as the size of the experimental SN grows). Nevertheless, to judge the true accuracy of the energy levels, the information contained in a tree (forest) is not sufficient as it is only through cycles that one can determine the true accuracy of the measurements (section 4). The network-theoretical view allows us to appreciate how (even-membered) cycles, containing a lot of extra information compared to, for example, minimum-weight spanning trees, within a component of an SN help to fix the energy levels and could tighten their uncertainties even below those of the original measurements.

3.12. Assigning Spectra. Assigning complicated high-resolution spectra is a major challenge; consequently, high-resolution spectroscopy is also a science (and art) of the quantum number assignment of measured lines. The techniques used evolved much over the years[90−96] but the end results is about the same: a high-resolution spectrum of a polyatomic molecule is converted to a list of labeled energies (Figure 3). When spectroscopists analyze high-resolution experimental spectra, they traditionally associate the lines with some good and mostly approximate quantum numbers followed by a fitting of the levels via a small number of spectroscopic parameters of a well-designed model Hamiltonian.[90] This type of assignment procedure fails in the case of highly excited rovibrational states and in general when the rovibrational transitions belong to congested areas of the observed spectrum and the subsequent analysis time exceeds an acceptable limit.

In ref 53 we advocated a novel protocol for the assignment of high-resolution one-photon absorption spectra based on the concept of SNs: detect the lines in a measured high-resolution spectrum leading to the largest number of new energy levels via an investigation of a suitable first-principles SN and assign the transitions with quantum numbers by mapping the *ab initio* line list onto experimental spectra using graph theory. Taking the negative logarithm of the intensity of the transitions as the weight function for the transitions of the SN, the minimum-weight spanning tree displays the transitions with the largest intensities; thus, it readily identifies the most intense and thus the practically most useful spectral features. Of course, this protocol could be combined with the traditional one to obtain the maximum amount of information from a spectrum with the least amount of effort.

4. MARVEL

From a practical point of view, at present probably the most important application of spectroscopic networks is their use within the MARVEL protocol,[49,50] where the acronym MARVEL stands for Measured Active Rotational−Vibrational Energy Levels.[48] Experimental energy levels originating from MARVEL investigations,[41−43,55−59,97,98] and the underlying set of assigned and measured transitions, can be accessed at the webpage http://ReSpecTh.hu. Note that there certainly exist approaches similar to MARVEL, including those developed by Flaud et al.[75] and Tashkun et al.[32]

The MARVEL approach is designed for a critical evaluation and consequent validation of experimental transition wavenumbers and uncertainties collected from the literature (Table 1), followed by the inversion of the wavenumber information to obtain the best possible set of energy levels with attached dependable uncertainties. Briefly, the MARVEL protocol includes the following steps: (1) Collection, preliminary validation, and compilation of all the available measured transitions possessing unambiguous labels and uncertainties into a database. (2) Determination of the distinct energy levels of the SN, built from the measured data collected. (3) Setting up a N_t-dimensional vector, $\mathbf{Y}$, containing the experimentally measured transitions, an $(N_l - 1)$-dimensional one, $\mathbf{X}$, containing the energy levels sought, and an extremely sparse matrix, $\mathbf{a}$, of dimension $N_t \times (N_l - 1)$, the Ritz-matrix, describing the relation between the transitions and the energy levels. (4) Least-squares solution of the system of linear equations obtained, including iterative improvement[99,100] of the experimental uncertainties if needed. In all these steps highly efficient algorithms are needed due to the large size of the SNs. These algorithms have been found;[50] thus, one iterative step in the MARVEL process, involving the formal inversion of a 100000 × 100000 matrix, takes less than a second on a single core.

The fundamental equations behind MARVEL are extremely simple. First, MARVEL is built upon the Ritz principle, which gives the connection between the measured transitions and the rovibronic energy levels:

$$\sigma_{ij} = E_i - E_j \tag{14}$$

where σ_{ij} is a measured wavenumber (ij = 1, ..., N_t), and E_j is a lower and E_i is an upper rovibronic energy level ($i, j \in 1, ..., N_l$). Let δ_{ij} be the measurement uncertainty of the σ_{ij} transition. Thus, the principal input to MARVEL is a grand list of N_t experimentally measured, assigned, and labeled transitions with corresponding uncertainties, and the aim of MARVEL is to determine the N_l energy levels with self-consistent uncertainties. An overdetermined system of linear equations,

$$\mathbf{aX} = \mathbf{Y} \tag{15}$$

characterizes all SNs. When weights $w_{ij} = \delta_{ij}^{-2}$ are introduced, we can write

$$\mathbf{AX} = \mathbf{B} \tag{16}$$

where $\mathbf{A} = \mathbf{a}^T\mathbf{wa}$ and $\mathbf{B} = \mathbf{a}^T\mathbf{wY}$, and the dimension of the extremely sparse $\mathbf{A}$ matrix is $(N_l - 1) \times (N_l - 1)$. Computation of $\mathbf{A}$ and $\mathbf{B}$ can be considerably accelerated by the use of analytic formulas.[50] Compressed row (CRS) or compressed column storage (CCS) formats[79] can be used to store the sparse $\mathbf{A}$ matrix very efficiently.

Solutions of an overdetermined system of linear equations have no meaning in an absolute sense; therefore, at least one of the energy levels needs to be fixed. SNs are rooted graphs; therefore, it is an obvious choice to fix the value of the lowest energy level, the root (or one of the roots of the PCs), and fix it to zero. Due to the nature of the experimental SNs, they may contain energy levels that have no path to the root; therefore, these energy levels must be identified before setting up the matrix equation. The fastest way to identify the components of the SN and to select nodes belonging to the same component

DOI: 10.1021/acs.jpca.6b02293
J. Phys. Chem. A 2016, 120, 8949−8969

of the SN is the DFS algorithm,[65,68] which significantly outperforms the Dijkstra algorithm[65] for this task.[101]

Both iterative and direct linear solver algorithms can be used to determine the MARVEL energy levels, *i.e.*, **X**. A considerable advantage of the direct methods is that the elements of the inverse matrix can be determined analytically. With $\mathbf{A}^{-1}$, the uncertainties (one standard deviation) of the energy levels can be computed as $\varepsilon_j \approx \sqrt{A_{jj}^{-1}}$. A considerable disadvantage of the direct methods is that they are much slower than the iterative algorithms. Because **A** is a symmetric positive definite matrix, we can use a sparse-adaptive $\mathbf{LDL}^{\mathrm{T}}$ decomposition as a special type of the Cholesky decomposition.[102] The robust reweighting algorithm[99] is especially well suited for the iterative adjustment of the uncertainties of the measured transitions. If approximate uncertainties are sufficient, like during the MARVEL iterations up to the final one to improve the experimental uncertainties, it is possible to use the preconditioned conjugate gradient method,[103−105] one of the fastest linear equation solvers. Features and performance of different algorithms tested to arrive at a highly efficient MARVEL code are summarized in Table 1 of ref 50.

4.1. Magic Numbers. As mentioned above, the absolute values of the MARVEL energy levels can only be determined if at least one energy level is fixed in the given SN. Most of the SNs, as prescribed by quantum mechanical selection rules, have more than one PC. One of these PCs contains the lowest energy level as root, whose value is chosen to be zero, with zero uncertainty. MARVEL cannot determine the absolute values of the lowest energy level of the other PCs, so we must link the PCs by so-called "magic numbers" to have absolute values for all the energies.

The value of the magic number can be estimated on the basis of empirical and/or theoretical considerations. The magic number can usually be deduced from a highly accurate empirical effective Hamiltonian. The experimental SN can also be used for the determination of magic numbers. This facility is provided by the observation that many molecules have degenerate energy pairs where the members of the pairs belong to different PCs (Figure 3). This may happen at only relatively high excitations and energies, but many of these excited states are usually amenable to experiments. These near degeneracies can be ascertained from accurate variational nuclear motion computations. Adding these artificial, zero-frequency "transitions" to the experimental SN the PCs become artificially connected and a refinement process can be initiated yielding the magic number. According to our experience,[42] the empirical magic number satisfies the experimental accuracy what is required during a MARVEL analysis.

4.2. Calibration. The databases that allow the execution of a MARVEL analysis contain all the measured transitions of a given molecule available from the literature, which means that these transitions have been measured over several decades under widely different experimental conditions, including pressure and temperature differences, using different spectrometers and different calibration standards. When these data are combined into a single database, systematic differences can be identified if several groups reported precise values with different accuracy and uncertainty estimates for the same transitions, yielding a multiedge SN. Inconsistencies may occur due to mistakes of different origin, but some of the inconsistencies, especially in the case of Fourier transform spectroscopy (FTS) measurements, are due to the use of different calibration standards recommended at different times.

The incorrectly calibrated FTS transitions can easily be corrected by applying a single multiplicative recalibration factor. However, this factor needs to be determined. An example is provided by the high-resolution spectroscopic data measured by Guelachvili for $H_2{}^{16}O$, and a couple of its isotopologues, and reported in 1983 in the 1066−2296 cm^{-1} region.[106] These data were revised about a decade later,[107] when Guelachvili et al. introduced a calibration factor of 0.99999977, improving substantially the accuracy of the measured lines. Although the deviation of this factor from 1.0 appears to be small, many FTS measurements have a relative accuracy considerably better than 10^{-7}, under ideal conditions this can be 10^{-9}−10^{-10}.

The base of the MARVEL determination of this multiplicative calibration factor is the minimization of the root-mean-square deviation between the FTS transitions scaled with a given factor and the MARVEL predicted transitions. Using the MARVEL calibration protocol we could determine basically the same calibration factor for $H_2{}^{16}O$ as determined by Guelachvili et al.[42] A similar situation was observed during the MARVEL studies of several other molecules.

4.3. Conflict of Highly Accurate Lines Measured for H_3^+. An interesting feasible application of network theory and MARVEL concerns the "planning" of experiments, *i.e.*, identification of unmeasured transition(s), which can result in new energy levels or solve an existing conflict among different measurements. A case in mind is when experimentalists claim higher accuracy than apparently their measurement has (or the accuracy is lowered substantially due to special circumstances, like the presence of strongly overlapping lines).

The following example considers a conflict between two sets[108,109] of highly accurate measured transitions of the molecular ion H_3^+. In 2013, two different groups studied the ν_2 band of H_3^+ and published highly accurate lines; however, their measured frequencies did not agree within the published uncertainties. Table 5 contains selected transitions from these

Table 5. Selected High-Quality Measured Transitions for H_3^+ from 13HoPeJeSi,[108] 13WuLiLiLi,[109] and 16JuKoScAs,[110] Showing Considerable Disagreement between the Former Two Measurements

transition	13HoPeJeSi[108]	13WuLiLiLi[109]	diff/10^{-5} cm^{-1}	16JuKoScAs[110]
$R(1,1)^l$	2691.44239(2)	2691.44305(33)	66	2691.442718(5)
$R(1,1)^u$	2726.21965(1)	2726.22025(66)	60	2726.220011(7)
$R(2,1)^u$	2826.11628(1)	2826.11683(33)	55	

two sources that exemplify the problem. The notation applied for the transitions of Table 5 is explained neither here nor in the table, the original sources should be consulted for this purpose. MARVEL and the SN approach in itself cannot solve this apparent conflict of the two measurements, *i.e.*, cannot select the "more accurate" transitions, because the energy levels involved in the conflict are not members of cycles. Nevertheless, the SN approach can predict, using the appropriate selection rules, accurate transitions that could create cycles among the energy levels involved in the problems. If it was feasible to measure these predicted transitions with an accuracy similar to those of the measurements of refs 108 and 109, then the cycle(s) created by the new measurements could fix the energy levels resolving the conflict. Figure 10 shows the

DOI: 10.1021/acs.jpca.6b02293
J. Phys. Chem. A 2016, 120, 8949−8969

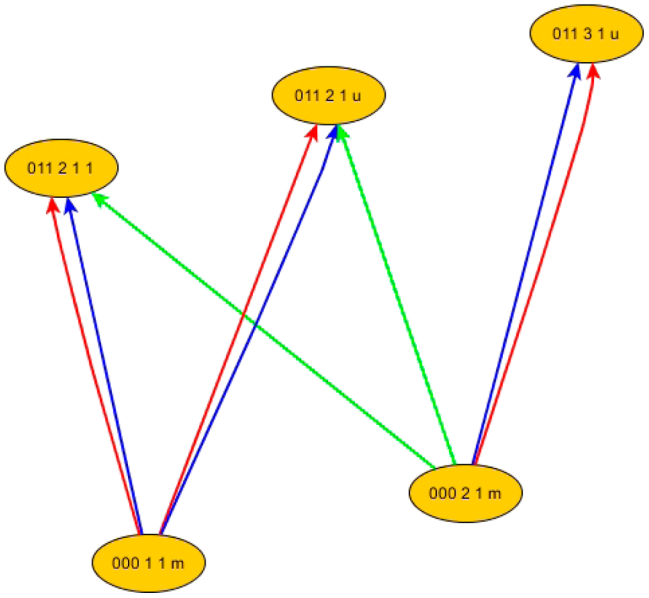

Figure 10. Part of the measured spectroscopic network of H_3^+ showing pictorially a conflict due to the accuracy of two sets of measurements: the red transitions were measured by 13HoPeJeSi[108] and the blue ones by 13WuLiLiLi.[109] The green, unmeasured transitions within the same measurable wavenumber range should help to solve the conflict of the two sets of measurements once and for all.

problem and the solution schematically. The blue and the red lines are the measured transitions (see also Table 5), and the green lines show the predicted MARVEL lines that appear in the region of feasible measurements and can create a cycle that could prove the accuracy of either one or the other original experimental study. During the revision of this paper a study from Asvany et al.[110] came to our attention, reporting improved, highly accurate lines for H_3^+. The results of ref 110 seem to indicate that McCall et al.[108] significantly overestimated the accuracy of their measurements, the results of Shy et al.,[109] reported with a higher uncertainty, agree within their uncertainty estimates with the high-precision results of Asvany et al.[110] Although the third set of transitions certainly help to point out problems with the earlier measurements, the final resolution of the conflict awaits for the determination of the transitions indicated in Figure 10.

4.4. Rovibronic States of $^{12}C_2$. $^{12}C_2$ is the only molecule among those studied by the MARVEL technique up to now where the transitions involve not rovibrational but mostly rovibronic states. Most significantly, the experimental spectroscopic measurements of $^{12}C_2$ involve three types of electronic states: singlet, triplet, and quintet. Therefore, it is not surprising that the experimental SN of $^{12}C_2$ is somewhat different from the experimental SNs of the other molecules studied by MARVEL.

The experimental SN of $^{12}C_2$ shown in Figure 11 has 16 Clauset−Newman−Moore (CNM)[80] clusters. This figure yields the following important information about the SN of $^{12}C_2$, some of which can also be applied to other SNs: (1) the CNM algorithm yields two principal clusters where the conjunctive transitions can immediately be recognized; (2) the two largest communities are formed principally by singlet and triplet energy levels, though not exclusively (this information is not shown in the figure); (3) most of the

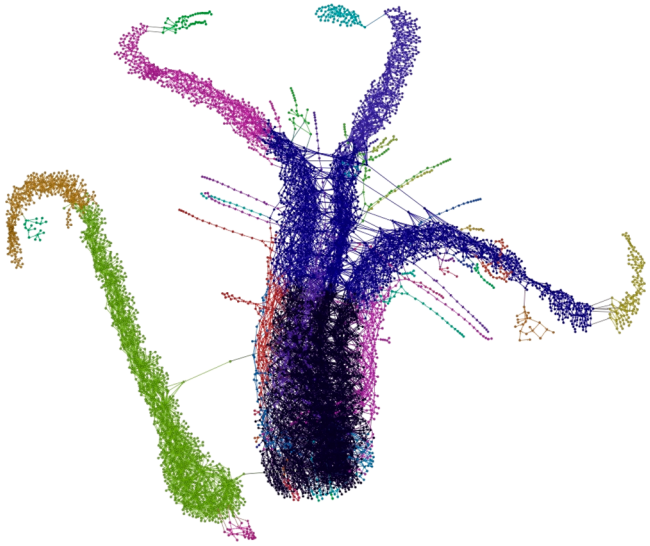

Figure 11. Clauset−Newman−Moore (CNM) clusters of the experimental spectroscopic network of the $^{12}C_2$ molecule.

communities with a small number of vertices are weakly connected to the main part of the SN; and (4) the larger communities contain a large number of cycles. The last statement is significant from the point of view of high-resolution spectroscopy, as it is tempting to believe that if a given energy level is part of at least one cycle then its value is well determined. This example shows that if the energy level is a member of a weakly connected cluster, then its uncertainty may depend strongly on the accuracy of transitions connecting the cluster to the main part of the SN. Therefore, the CNM method can be used to detect small communities, in which the uncertainties of the energy levels may reflect this weakly connected property. This figure also nicely shows the large number of branches almost always characteristic of experimental SNs.

5. SUMMARY AND CONCLUSIONS

Driven by the need of scientific and engineering applications, information systems containing line-by-line high-resolution spectroscopic data have become ubiquitous during the last 20 years or so. These information systems contain rovibronic transitions for a considerable number of small molecules, selected on the basis of the need of the applications, usually containing two to six atoms. The largest of the computed line lists have up to 10^{10} transitions,[111,112] clearly calling for "big data" techniques to generate, store, validate, distribute, and utilize the information. It must be emphasized that although quantum chemical computations are able to yield the complete set of the required line-by-line information even for semirigid pentatomic molecules, like $^{12}CH_4$,[112] the accuracy of the line positions is limited and thus should be replaced by much more accurate experimental data whenever they are available. As emphasized in this article, to make maximum use of the experimental spectroscopic line list information, the grand list of measured spectroscopic transitions of a molecule should be viewed as a weighted, undirected, and rooted graph, a spectroscopic network (SN). The vertices of the SN are the energy levels (these are principally independent of the type of measurement providing them), whereas the edges are the spectroscopically allowed transitions and the weights are the transition intensities (both depend on the type of measurement

DOI: 10.1021/acs.jpca.6b02293
J. Phys. Chem. A 2016, 120, 8949−8969

performed). Obviously, transition intensities have a crucial role in determining the structure of SNs and different spectroscopic techniques yield SNs with drastically different topologies.

Experiments yield relatively small multiedge random graphs: the largest experimental SN studied, that of *ortho*- and *para*-$H_2{}^{16}O$,[42] contains about 20000 energy levels and 200000 transitions, of which about 100000 are unique. A given first-principles computation of rovibronic energy levels and spectra results in a very large deterministic simple graph.

The network-theoretical view of the results of high-resolution spectroscopy experiments yielding rovibronic transitions and energy levels, after introducing the concept of spectroscopic networks (SN) and once one understands the structure of the SNs, offers several concepts and tools toward the complete characterization of the related rovibronic energies and spectra, some of which can be summarized as follows:

(1) SNs of simple molecules usually contain more than one principal component (PC), as required by nuclear spin statistics. PCs are giant components of the spectroscopic networks. Experimental spectroscopic networks occasionally contain floating components, whose energy levels are not attached to any of the energy levels of the PCs. Unification of the components of an experimental SN is important to obtain "absolute" energy values for the vertices of components disjoint from the PCs.

(2) The degree distribution of all experimental SNs investigated turns out to be free of a scale. The scale-free property of the overall network degree distribution of SNs thus established leads to the useful concept of hubs, *i.e.*, the emergence of a relatively few energy levels with a relatively large number of transitions. Note that this statement is independent of the assumed degree distribution of SNs; it only relies on the heavy-tail distribution observed in all cases. The established existence of hubs provides design ideas for highly useful spectroscopic measurements. For example, accurate measurement of transitions involving the least well characterized hubs of the experimental SN leads straightforwardly to a more accurate list of levels and lines.

(3) The fact that the PCs of experimental SNs are giant components can be explained by the observation that all experimental SNs studied exhibit heavy tails in their degree distribution with the exponent of the assumed fitted power-law distribution of about 2.2. This scaling index means, according to modeling studies,[7] that the SNs are allowed to have giant components and small ones occur only occasionally. This is a useful property of spectroscopic networks as it ensures that most of the rovibronic energy levels can be obtained from a diverse set of experimental measurements.

(4) All the experimental spectroscopic networks investigated turn out to be bipartite. This is another important property of SNs. It reflects the fact that the parity of the energy levels has to change during experimentally measurable one-photon transitions. The bipartite nature of SNs means that SNs contain only even-membered cycles, the smallest possible cycle involves four energy levels. Bipartiteness allows, for example, for a simple partial check of the correctness of the labels of the lines listed in spectroscopic databases.

(5) Detailed investigation of first-principles SNs show that, although the great majority of the transitions is extremely weak, it is possible to find a few relatively strong transitions for almost all energy levels. This suggests that with relatively standard spectroscopic techniques almost all of the bound rovibronic energy levels can be determined through measurement of transitions they are involved in.

(6) Detailed comparison of measured and computed hubs helps to determine the weakest links within an experimental SN, *i.e.*, those transitions that are least well determined and whose accurate knowledge is most important to ensure the overall accuracy of the lines and levels involved in the SN.

(7) It seems that the PageRank order[76] of the hubs can be significantly different from their degree order. PageRank provides the more useful measure as within the PageRank ordering system hubs are preferentially connected with hubs.

(8) The scale-free spectroscopic networks are robust against random removal of nodes. The robust structure of the experimental spectroscopic networks investigated means that they have a small diameter, resulting in the ultrasmall-world property of SNs.

(9) The matrix representations of SNs, involving the adjacency, and the combinatorial and normalized Laplacians, can be used to learn a number of details about the structure of the experimental spectroscopic networks. Most of the times the same information can be obtained by other means, but for the clustering of SNs the normalized Laplacian seems to offer the best opportunity. It is tempting to believe that a rovibronic energy level is experimentally well determined if it is part of a cycle. Clustering methods, some relying on matrix representations of SNs, help to detect small communities of rovibronic energy levels in which the uncertainties of the energy levels should reflect this weakly connected property.

(10) Besides model Hamiltonians with a relatively small number of parameters, another opportunity to reduce spectroscopic data to manageable size is the conversion of rovibronic transitions into rovibronic energy levels. Minimum-weight spanning trees, where the weights are defined by transition intensities, comprise the minimum amount of transition information needed to represent the experimentally available energy levels.

(11) In a high-resolution study a spectrum of a polyatomic molecule is converted into a list of labeled energy levels. Among other techniques, this can be achieved very efficiently via the use of the minimum-weight spanning tree, as it identifies the most intense and thus practically most useful spectral features.

Probably the most important application of the concept of spectroscopic networks is their use within the MARVEL (Measured Active Rotational−Vibrational Energy Levels) procedure yielding rovibronic energy levels, referenced to a selected zero level, from measured transitions involving them. The MARVEL code is not only completely general and can be applied to any molecule but also is very fast, allowing on-the-fly analysis of arbitrary experimental SNs and experimental spectra. MARVEL has been used to study the experimental energy level structure of 15 molecules[40−43,55−59] and yielded tens of

DOI: 10.1021/acs.jpca.6b02293
J. Phys. Chem. A 2016, 120, 8949−8969

thousands of highly accurate energy levels. In favorable cases MARVEL allows the "experimental" determination of the energy difference between the roots of the principal components of experimental SNs, through degeneracies of (highly excited) energy levels belonging to different principal components. MARVEL also facilitates the calibration of Fourier-transform spectroscopy studies, an important feature when transitions from many different experimental sources must be used together. As shown for example for H_3^+, the network-theoretical view of molecular spectra helps to understand conflicts of existing experiments and to propose new experiments to resolve the contradictions.

Spectroscopic networks, perhaps as part of active databases, are expected to become an intrinsic part of the description of high-resolution spectra of molecules. Nevertheless, investigation of large-scale SNs, containing hundreds of thousands of nodes and hundreds of millions of links calls for further improvements in the mathematical algorithms and tools of network theory.

We have shown that quantum mechanics builds complex networks highly similar to man-made ones. The popular notions of interdisciplinary scientific, social, and communication network investigations, like the scale-free and "small world" properties, hubs, network dynamics, self-organization, robustness, and attack/error tolerance, are all relevant when experimental (and to some extent first principles) spectroscopic networks are characterized.

AUTHOR INFORMATION

Corresponding Author

*A. G. Császár. Phone: +36-1-372-2929. E-mail: csaszar@chem.elte.hu.

Notes

The authors declare no competing financial interest.

ACKNOWLEDGMENTS

The project was supported by NKFIH (grant no. NK83583). The authors gratefully acknowledge the many useful discussions related to the topic of this article with Dr. Marianna Bolla, Dr. Beáta Faller, Prof. László Lovász, Dr. Edit Mátyus, Dr. Georg Mellau, Prof. Jonathan Tennyson, and Dr. János Tóth. The support received via the COST Action CM1405, MOLIM: Molecules in Motion, is also acknowledged.

REFERENCES

(1) Euler, L. The seven bridges of Königsberg. *Commentarii academiae scientiarum Petropolitanae* **1741**, *8*, 128−140.

(2) Hinde, A. J. *The development of modern chemistry*; Dover: New York, 1984.

(3) Interestingly, graph theory owes its name to chemistry, as the "graphical notation" or "chemicograph" of chemical species abundantly used in the 19th century, and pioneered by Brown and Kekulé, was abbreviated by the noted mathematician John Joseph Sylvester to "graphs" in 1878, see: Sylvester, J. J. Chemistry and algebra. *Nature* **1878**, *17*, 284.

(4) Barabási, A.-L.; Albert, R. Emergence of scaling in random networks. *Science* **1999**, *286*, 509−512.

(5) Albert, R.; Barabási, A.-L. Statistical mechanics of complex networks. *Rev. Mod. Phys.* **2002**, *74*, 47−97.

(6) Boccaletti, S.; Latora, V.; Moreno, Y.; Chavez, M.; Hwang, D.-U. Complex networks: Structure and dynamics. *Phys. Rep.* **2006**, *424*, 175−308.

(7) Newman, M. E. J. *Networks*; Oxford University Press: Oxford, U.K., 2010.

(8) Albert, R.; Jeong, H.; Barabási, A.-L. Error and attack tolerance of complex networks. *Nature* **2000**, *406*, 378−382.

(9) Jeong, H.; Tombor, B.; Albert, R.; Oltvai, Z. N.; Barabási, A.-L. The large-scale organization of metabolic networks. *Nature* **2000**, *407*, 651−654.

(10) Jeong, H.; Mason, S.; Barabási, A.-L.; Oltvai, Z. N. Lethality and centrality in protein networks. *Nature* **2001**, *411*, 41−42.

(11) Albert, R.; Jeong, H.; Barabási, A.-L. Diameter of the world-wide web. *Nature* **1999**, *401*, 130−131.

(12) Li, L.; Alderson, D.; Doyle, J. C.; Willinger, W. Towards a theory of scale-free graphs: Definition, properties, and implications. *Internet Math.* **2005**, *2*, 431−523.

(13) Barabási, A.-L.; Ravasz, E.; Vicsek, T. Deterministic scale-free networks. *Phys. A* **2001**, *299*, 559−564.

(14) Tennyson, J.; Yurchenko, S. N. ExoMol: Molecular line lists for exoplanet and other atmospheres. *Mon. Not. R. Astron. Soc.* **2012**, *425*, 21−33.

(15) Barber, R. J.; Tennyson, J.; Harris, G. J.; Tolchenov, R. N. A high accuracy computed water line list. *Mon. Not. R. Astron. Soc.* **2006**, *368*, 1087−1094.

(16) Voronin, B. A.; Tennyson, J.; Tolchenov, R. N.; Lugovskoy, A. A.; Yurchenko, S. N. A high accuracy computed line list for the HDO molecule. *Mon. Not. R. Astron. Soc.* **2010**, *402*, 492−496.

(17) Brown, L. R.; Farmer, C. B.; Rinsland, C. P.; Toth, R. A. Molecular line parameters for the atmospheric trace molecule spectroscopy experiment. *Appl. Opt.* **1987**, *26*, 5154−5182.

(18) Babikov, Y.; Mikhailenko, S.; Barbe, A.; Tyuterev, V. S&MPO − An information system for ozone spectroscopy on the WEB. *J. Quant. Spectrosc. Radiat. Transfer* **2014**, *145*, 169−196.

(19) Tyuterev, Vl. G.; Babikov, Yu. L.; Tashkun, S. A.; Perevalov, V. I.; Nikitin, A.; Champion, J.-P.; Wenger, Ch.; Pierre, C.; Pierre, G.; Hilico, J.-C.; Loete, M. T.D.S. spectroscopic databank for spherical tops: DOS version. *J. Quant. Spectrosc. Radiat. Transfer* **1994**, *52*, 459−480.

(20) Wenger, C.; Champion, J. Spherical top data system (STDS) software for the simulation of spherical top spectra. *J. Quant. Spectrosc. Radiat. Transfer* **1998**, *59*, 471−480.

(21) Wenger, C.; Boudon, V.; Rotger, M.; Sanzharov, M.; Champion, J. P. XTDS and SPVIEW: Graphical tools for the analysis and simulation of high-resolution molecular spectra. *J. Mol. Spectrosc.* **2008**, *251*, 102−113.

(22) Ba, Y. A.; Wenger, Ch.; Surleau, R.; Boudon, V.; Rotger, M.; Daumont, L.; Bonhommeau, D. A.; Tyuterev, V. G.; Dubernet, M.-L. MeCaSDa and ECaSDa: Methane and ethene calculated spectroscopic databases for the virtual atomic and molecular data centre. *J. Quant. Spectrosc. Radiat. Transfer* **2013**, *130*, 62−68.

(23) Tashkun, S.; Perevalov, V. CDSD-4000: high-resolution, high-temperature carbon dioxide spectroscopic databank. *J. Quant. Spectrosc. Radiat. Transfer* **2011**, *112*, 1403−1410.

(24) Rothman, L. S. The evolution and impact of the HITRAN molecular spectroscopic database. *J. Quant. Spectrosc. Radiat. Transfer* **2010**, *111*, 1565−1567.

(25) Rothman, L. S.; Gordon, I. E.; Babikov, Y.; Barbe, A.; Chris Benner, D.; Bernath, P. F.; Birk, M.; Bizzocchi, L.; Boudon, V.; Brown, L. R.; et al. The HITRAN2012 molecular spectroscopic database. *J. Quant. Spectrosc. Radiat. Transfer* **2013**, *130*, 4−50.

(26) Rothman, L. S.; Gordon, I. E.; Barber, R. J.; Dothe, H.; Gamache, R. R.; Goldman, A.; Perevalov, V. I.; Tashkun, S. A.; Tennyson, J. HITEMP, the high-temperature molecular spectroscopic database. *J. Quant. Spectrosc. Radiat. Transfer* **2010**, *111*, 2139−2150.

(27) Jacquinet-Husson, N.; Crepeau, L.; Armante, R.; Boutammine, C.; Chédin, A.; Scott, N. A.; Crevoisier, C.; Capelle, V.; Boone, C.; Poulet-Crovisier, N.; et al. The 2009 edition of the GEISA spectroscopic database. *J. Quant. Spectrosc. Radiat. Transfer* **2011**, *112*, 2395−2445.

(28) Müller, H. S. P.; Schlöder, F.; Stutzki, J.; Winnewisser, G. The Cologne database for molecular spectroscopy, CDMS: a useful tool for astronomers and spectroscopists. *J. Mol. Struct.* **2005**, *742*, 215−227.

DOI: 10.1021/acs.jpca.6b02293
J. Phys. Chem. A 2016, 120, 8949−8969

(29) Müller, H. S. P.; Thorwirth, S.; Roth, D. A.; Winnewisser, G. The Cologne database for molecular spectroscopy, CDMS. *Astron. Astrophys.* **2001**, *370*, L49−L52.
(30) Müller, H. S. P.; Endres, C. P.; Stutzki, J.; Schlemmer, S. The CDMS view on molecular data needs of Hershel, SOFIA, and ALMA. *AIP Conf. Proc.* **2012**, *1545*, 96−109.
(31) Pickett, H. M.; Poynter, R. L.; Cohen, E. A.; Delitsky, M. L.; Pearson, J. C.; Müller, H. S. P. Submillimeter, millimeter, and microwave spectral line catalog. *J. Quant. Spectrosc. Radiat. Transfer* **1998**, *60*, 883−890.
(32) Tashkun, S. A.; Perevalov, V. I.; Teffo, J.-L.; Bykov, A. D.; Lavrentieva, N. N. CDSD-1000, the high-temperature carbon dioxide spectroscopic databank. *J. Quant. Spectrosc. Radiat. Transfer* **2003**, *82*, 165−196.
(33) Dere, K. P.; Landi, E.; Young, P. R.; Del Zanna, G.; Landini, M.; Mason, H. E. CHIANTI − an atomic database for emission lines. IX. Ionization rates, recombination rates, ionization equilibria for the elements hydrogen through zinc and updated atomic data. *Astron. Astrophys.* **2009**, *498*, 915−929.
(34) Erdős, P.; Rényi, A. On random graphs. I. *Publ. Math.* **1959**, *6*, 290−297.
(35) Erdős, P.; Rényi, A. On the evolution of random graphs. *Publ. Math. Inst. Hung. Acad. Sci.* **1960**, *5*, 17−61.
(36) Erdős, P.; Rényi, A. On the strength of connectedness of a random graph. *Acta Math. Acad. Sci. Hung.* **1964**, *12*, 261−267.
(37) Bollobás, B. *Random graphs*; Academic Press: New York, 1985.
(38) Bollobás, B. *Modern graph theory*; Springer: New York, 1998.
(39) Forst, W. *Unimolecular reactions. A concise introduction*; Cambridge University Press: Cambridge, U.K., 2003.
(40) Tennyson, J.; Bernath, P. F.; Brown, L. R.; Campargue, A.; Carleer, M. R.; Császár, A. G.; Gamache, R. R.; Hodges, J. T.; Jenouvrier, A.; Naumenko, O. V.; et al. V. IUPAC critical evaluation of the rotational-vibrational spectra of water vapor. Part I. Energy levels and transition wavenumbers for $H_2{}^{17}O$ and $H_2{}^{18}O$. *J. Quant. Spectrosc. Radiat. Transfer* **2009**, *110*, 573−596.
(41) Tennyson, J.; Bernath, P. F.; Brown, L. R.; Campargue, A.; Carleer, M. R.; Császár, A. G.; Daumont, L.; Gamache, R. R.; Hodges, J. T.; Jenouvrier, A.; et al. IUPAC critical evaluation of the rotational-vibrational spectra of water vapor. Part II. Energy levels and transition wavenumbers for $HD^{16}O$, $HD^{17}O$, and $HD^{18}O$. *J. Quant. Spectrosc. Radiat. Transfer* **2010**, *111*, 2160−2184.
(42) Tennyson, J.; Bernath, P. F.; Brown, L. R.; Campargue, A.; Császár, A. G.; Daumont, L.; Gamache, R. R.; Hodges, J. T.; Naumenko, O. V.; Polyansky, O. L.; et al. Lodi, L.; Mizus, I. I. IUPAC critical evaluation of the rotational-vibrational spectra of water vapor. Part III. Energy levels and transition wavenumbers for $H_2{}^{16}O$. *J. Quant. Spectrosc. Radiat. Transfer* **2013**, *117*, 29−58.
(43) Tennyson, J.; Bernath, P. F.; Brown, L. R.; Campargue, A.; Császár, A. G.; Daumont, L.; Gamache, R. R.; Hodges, J. T.; Naumenko, O. V.; Polyansky, O. L.; et al. IUPAC critical evaluation of the rotational-vibrational spectra of water vapor. Part IV. Energy levels and transition wavenumbers for $D_2{}^{16}O$, $D_2{}^{17}O$, and $D_2{}^{18}O$. *J. Quant. Spectrosc. Radiat. Transfer* **2014**, *142*, 93−108.
(44) Bunker, P. R.; Jensen, P. *Molecular symmetry and spectroscopy*, 2nd ed.; NRC Research Press: Ottawa, 1998.
(45) Mellau, G. Ch Complete experimental rovibrational eigenenergies of HNC up to 3743 cm^{-1} above the ground state. *J. Chem. Phys.* **2010**, *133*, 164303.
(46) Mellau, G. Ch Complete experimental rovibrational eigenenergies of HCN up to 6880 cm^{-1} above the ground state. *J. Chem. Phys.* **2011**, *134*, 234303.
(47) Mellau, G. Ch Rovibrational eigenenergy structure of the [H,C,N] molecular system. *J. Chem. Phys.* **2011**, *134*, 194302.
(48) Császár, A. G.; Czakó, G.; Furtenbacher, T.; Mátyus, E. An active database approach to complete spectra of small molecules. *Annu. Rep. Comput. Chem.* **2007**, *3*, 155−176.
(49) Furtenbacher, T.; Császár, A. G.; Tennyson, J. MARVEL: measured active rotational-vibrational energy levels. *J. Mol. Spectrosc.* **2007**, *245*, 115−125.
(50) Furtenbacher, T.; Császár, A. G. MARVEL: measured active rotational-vibrational energy levels. II. Algorithmic improvements. *J. Quant. Spectrosc. Radiat. Transfer* **2012**, *113*, 929−935.
(51) Császár, A. G.; Furtenbacher, T. Spectroscopic networks. *J. Mol. Spectrosc.* **2011**, *266*, 99−103.
(52) Furtenbacher, T.; Császár, A. G. The role of intensities in determining characteristics of spectroscopic networks. *J. Mol. Struct.* **2012**, *1009*, 123−129.
(53) Furtenbacher, T.; Árendás, P.; Mellau, G.; Császár, A. G. Simple molecules as complex systems. *Sci. Rep.* **2014**, *4*, 4654.
(54) Árendás, P.; Furtenbacher, T.; Császár, A. G. On spectra of spectra. *J. Math. Chem.* **2016**, *54*, 806−822.
(55) Fábri, C.; Mátyus, E.; Furtenbacher, T.; Mihály, B.; Zoltáni, T.; Nemes, L.; Császár, A. G. Variational quantum mechanical and active database approaches to the rotational-vibrational spectroscopy of ketene. *J. Chem. Phys.* **2011**, *135*, 094307.
(56) Furtenbacher, T.; Szidarovszky, T.; Mátyus, E.; Fábri, C.; Császár, A. G. Analysis of the rotational-vibrational states of the molecular ion H_3^+. *J. Chem. Theory Comput.* **2013**, *9*, 5471−5478.
(57) Furtenbacher, T.; Szidarovszky, T.; Fábri, C.; Császár, A. G. MARVEL analysis of the rotational-vibrational states of the molecular ions H_2D^+ and D_2H^+. *Phys. Chem. Chem. Phys.* **2013**, *15*, 10181−10193.
(58) Al Derzi, A. R.; Furtenbacher, T.; Tennyson, J.; Yurchenko, S. N.; Császár, A. G. MARVEL analysis of the measured high-resolution spectra of $^{14}NH_3$. *J. Quant. Spectrosc. Radiat. Transfer* **2015**, *161*, 117−130.
(59) Furtenbacher, T.; Szabó, I.; Császár, A. G.; Bernath, P. F.; Yurchenko, S. N.; Tennyson, J. Experimental energy levels and the related high-temperature partition function of the $^{12}C_2$ molecule. *Astrophys. J. Suppl.* **2016**, *224*, 44.
(60) Tennyson, J.; Bernath, P. F.; Brown, L. R.; Campargue, A.; Császár, A. G.; Daumont, L.; Gamache, R. R.; Hodges, J. T.; Naumenko, O. V.; Polyansky, O. L.; et al. A database of water transitions from experiment and theory (IUPAC technical report). *Pure Appl. Chem.* **2014**, *86*, 71−83.
(61) Polyansky, O. L.; Császár, A. G.; Shirin, S. V.; Zobov, N. F.; Barletta, P.; Tennyson, J.; Schwenke, D. W.; Knowles, P. J. High-accuracy ab initio rotation-vibration transitions for water. *Science* **2003**, *299*, 539−542.
(62) Császár, A. G.; Fábri, C.; Szidarovszky, T.; Mátyus, E.; Furtenbacher, T.; Czakó, G. Fourth age of quantum chemistry: Molecules in motion. *Phys. Chem. Chem. Phys.* **2012**, *14*, 1085−1106.
(63) Tennyson, J. Accurate variational calculations for line lists to model the vibration-rotation spectra of hot astrophysical objects. *WIREs Comput. Mol. Sci.* **2012**, *2*, 698−715.
(64) Bowman, J. M.; Carrington, T.; Meyer, H.-D. Variational quantum approaches for computing vibrational energies of polyatomic molecules. *Mol. Phys.* **2008**, *106*, 2145−2182.
(65) Diestel, R. *Graph theory*, 3rd ed.; Springer: Berlin, 2005.
(66) Harary, F. *Graph theory*; Addison-Wesley: Reading, MA, 1969.
(67) Wilson, R. J. *Introduction to graph theory*, 3rd ed.; Longman: Harlow, 1985.
(68) Sedgewick, R. ed. *Algorithms in C++. Part 5: Graph algorithms*; Addison-Wesley: Reading, MA, 2002.
(69) Kruskal, J. B. On the shortest spanning subtree of a graph and the traveling salesman problem. *Proc. Am. Math. Soc.* **1956**, *7*, 48−50.
(70) Note that a one-dimensional quantum harmonic oscillator has an infinite number of energy levels but only one transition wavenumber allowed by quantum mechanical selection rules of one-photon transitions.
(71) Kirchhoff, G. Über die Auflösung der Gleichingen, auf welche man bei der untersuchung der linearen verteilung galvanischer Strömegeführt wird. *Ann. Phys.* **1847**, *148*, 497−508.
(72) Chaiken, S. A combinatorial proof of the all-minors matrix tree theorem. *SIAM J. Alg. Disc. Methods* **1982**, *3*, 319−329.
(73) Bolla, M. *Spectral clustering and biclustering: Learning large graphs and contingency tables*; Wiley: New York, 2013.

DOI: 10.1021/acs.jpca.6b02293
J. Phys. Chem. A 2016, 120, 8949−8969

(74) Bolla, M. Penalized versions of the Newman-Girvan modularity and their relation to normalized cuts and *k*-means clustering. *Phys. Rev. E* **2011**, *84*, 016108.
(75) Flaud, J.-M.; Camy-Peyret, C.; Maillard, J. P. Higher rovibrational levels of H_2O deduced from high resolution oxygen-hydrogen flame spectra between 2800−6200 cm^{-1}. *Mol. Phys.* **1976**, *32*, 499−521.
(76) Brin, S.; Page, I. The anatomy of a large-scale hypertextual web search engine. *Comput. Netw. ISDN Syst.* **1998**, *30*, 107−117.
(77) Ghoshal, G.; Barabási, A.-L. Ranking stability and super-stable nodes in complex networks. *Nat. Commun.* **2011**, *2*, 394.
(78) Newman, M. E. J. Assortative mixing in networks. *Phys. Rev. Lett.* **2002**, *89*, 208701.
(79) Fortunato, S. Community detection in graphs. *Phys. Rep.* **2010**, *486*, 75−174.
(80) Clauset, A.; Newman, M. E. J.; Moore, C. Finding community structure in very large networks. *Phys. Rev. E* **2004**, *70*, 066111.
(81) http://snap.stanford.edu/snap/, last accessed on February 18, 2016.
(82) Schmidt, J. M. A simple test on 2-vertex- and 2-edge-connectivity. *Inform. Proc. Lett.* **2013**, *113*, 241−244.
(83) Császár, A. G.; Furtenbacher, T. Promoting and inhibiting tunneling via nuclear motions. *Phys. Chem. Chem. Phys.* **2016**, *18*, 1092−1104.
(84) Miani, A.; Tennyson, J. Can ortho-para transitions for water be observed? *J. Chem. Phys.* **2004**, *120*, 2732−2739.
(85) Kroto, H. W. *Molecular rotation spectra*; Wiley: New York, 1975.
(86) Molloy, M.; Reed, B. A critical point for random graphs with a given degree sequence. *Random Struct. Alg.* **1995**, *6*, 161−179.
(87) Aiello, W.; Chung, F.; Lu, L. A random graph model for massive graphs, in *Proceedings of the 32nd Annual ACM Symposium on Theory of Computing*; Association of Computing Machinery: New York, 2000; pp 171−180.
(88) Barabási, A.-L. *Linked*; Perseus: Cambridge, U.K., 2002.
(89) Mohar, B. Some applications of Laplace eigenvalues of graphs. http://www.fmf.uni-lj.si/~mohar/Papers/Montreal.pdf, 1997.
(90) Watson, J. K. G. In *Vibrational spectra and structure*; Durig, J. R., Ed.; Elsevier: Amsterdam, 1977; Vol. *6*, Chapter 1.
(91) van Wijngaarde, J.; Desmond, D.; Meerts, W. L. Analysis of high resolution FTIR spectra from synchrotron sources using evolutionary algorithms. *J. Mol. Spectrosc.* **2015**, *315*, 107−113.
(92) Meerts, W. L.; Schmitt, M. Application of genetic algorithms in automated assignments of high-resolution spectra. *Int. Rev. Phys. Chem.* **2006**, *25*, 353−406.
(93) Loomis, F. W.; Wood, R. W. The rotational structure of the blue-green bands of Na_2. *Phys. Rev.* **1928**, *32*, 223−236.
(94) Kisiel, Z.; Pszczolkowski, L.; Medvedev, I. R.; Winnewisser, M.; Lucia, F.; Herbst, C. E. Rotational spectrum of trans-trans diethyl ether in the ground and three excited vibrational states. *J. Mol. Spectrosc.* **2005**, *233*, 231−243.
(95) Moruzzi, G.; Xu, L.-H.; Lees, R. M.; Winnewisser, B. P.; Winnewisser, M. Investigation of the ground vibrational state of CD_3OH by a new "Ritz" program for direct energy level fitting. *J. Mol. Spectrosc.* **1994**, *167*, 156−175.
(96) Helm, R. M.; Vogel, H.-P.; Neusser, H. J. Highly resolved UV spectroscopy: structure of S_1 benzonitrile and benzonitrile-argon by correlation automated rotational fitting. *Chem. Phys. Lett.* **1997**, *270*, 285−292.
(97) Furtenbacher, T.; Császár, A. G. On employing $H_2{}^{16}O$, $H_2{}^{17}O$, $H_2{}^{18}O$, and $D_2{}^{16}O$ lines as frequency standards in the 15−170 cm^{-1} window. *J. Quant. Spectrosc. Radiat. Transfer* **2008**, *109*, 1234−1251.
(98) Császár, A. G.; Furtenbacher, T. Promoting and inhibiting tunneling via nuclear motions. *Phys. Chem. Chem. Phys.* **2016**, *18*, 1092−1104.
(99) Watson, J. K. G. Robust weighting in least-squares fits. *J. Mol. Spectrosc.* **2003**, *219*, 326−328.
(100) Bai, Z., Demmel, J., Dongarra, J., Ruhe, A., van der Vorst, H., Eds. *Templates for the solution of algebraic eigenvalue problems: a practical guide*; Society for Industrial and Applied Mathematics: Philadelphia, PA, 2000.
(101) It must be emphasized that if we want to examine certain properties of the SN, such as the diameter, the Dijkstra algorithm appears to be an excellent choice.
(102) Dahlqvist, G.; Björck, A. *Numerical methods*; Dover: New York, 2003.
(103) Golub, G. H.; Loan, C. F. *Matrix computations*; The Johns Hopkins University Press: Boston, 1996.
(104) Paige, C. C.; Saunders, M. A. Algorithm 583. LSQR: sparse linear equations and least squares problems. *ACM Trans. Math. Softw.* **1982**, *8*, 43−71.
(105) Paige, C. C.; Saunders, M. A. LSQR: An algorithm for sparse linear equations and sparse least squares. *ACM Trans. Math. Softw.* **1982**, *8*, 195−209.
(106) Guelachvili, G. Experimental Doppler-limited spectra of the ν_2-bands of $H_2{}^{16}O$, $H_2{}^{17}O$, $H_2{}^{18}O$, and HDO by Fourier-transform spectroscopy − secondary wave-number standards between 1066 and 2296 cm^{-1}. *J. Opt. Soc. Am.* **1983**, *73*, 137−50.
(107) Guelachvili, G.; Birk, M.; Borde, C. J.; Brault, J. W.; Brown, L. R.; Carli, B.; et al. High resolution wavenumber standards for the infrared. *J. Mol. Spectrosc.* **1996**, *177*, 164−79.
(108) Hodges, J. N.; Perry, A. J.; Jenkins, P. A.; Siller, B. M.; McCall, B. J. High-precision and high-accuracy rovibrational spectroscopy of molecular ions. *J. Chem. Phys.* **2013**, *139*, 164201.
(109) Wu, K.-Y.; Lien, Y.-H.; Liao, C.-C.; Lin, Y.-R.; Shy, J.-T. Measurement of the ν_2 fundamental band of H_3^+. *Phys. Rev. A: At., Mol., Opt. Phys.* **2013**, *88*, 032507.
(110) Jusko, P.; Konietzko, C.; Schlemmer, S.; Asvany, O. Frequency comb assisted measurement of fundamental transitions of cold H_3^+, H_2D^+ and D_2H^+. *J. Mol. Spectrosc.* **2016**, *319*, 55−58.
(111) Yurchenko, S. N.; Barber, R. J.; Tennyson, J. A variationally computed line list for hot NH_3. *Mon. Not. R. Astron. Soc.* **2011**, *413*, 1828−1834.
(112) Yurchenko, S. N.; Tennyson, J.; Bailey, J.; Hollis, M. D. J.; Tinetti, G. Spectrum of hot methane in astronomical objects using a comprehensive computed line list. *Proc. Natl. Acad. Sci. U. S. A.* **2014**, *111*, 9379−9383.

DOI: 10.1021/acs.jpca.6b02293
J. Phys. Chem. A 2016, 120, 8949−8969